Interactive comment on "Biogeophysical impacts of peatland forestation on regional climate changes in Finland" by Y. Gao et al.

We deeply appreciate all the reviewers for their constructive comments in improving the scientific quality of this manuscript. Our point-by-point response to all the reviewers' comments are listed below, and corresponding modifications are also made for the manuscript. We hope our reply will satisfy the expectations from reviewers.

Response to Anonymous Referee #1

General comments:

I commend the authors for a timely study about effects of human actions on the climate system. The paper describes how the representation of vegetation in the calculation cells of the REMO model have been improved with the aid of the data of the Finnish National Forest Inventory (FNFI). This allows for estimating the effects of peatland drainage (that allows tree growth, that is, forestation) by using results of two inventories, between which a substantial change has occurred. My expertise is forest modeling, I am not able to judge the details of application of the REMO model.

The results are derived from two 18 year long simulations with REMO that use vegetation cover data from two FNFI measurements. The main finding is that peatland forestation results in strong spring warming that is highly heterogeneous spatially and temporally. There are also effects on albedo, precipitation and net surface radiation throughout the year.

The results compare favorably to some observations. They are presented and discussed somewhat from the point of view of their sensitivity to input data and parameter values. However, the paper would be even better if a more comprehensive sensitivity analysis had been made by additional model runs. For example:

- The paper discusses uncertainties in background albedo values (l. 527- 558)

- Local effects of peatland forestation areas on maximum net surface solar difference (l. 503-525)

- Uncertainties in translating FNFI cover information to a compatible form with REMO (l. 220-224)

Authors response (AR): Systematically changing surface parameters, such as background albedo, may help to test the robustness of simulation results. However, it requires heavy computing to do this kind of sensitivity test with a regional climate model, which makes it not really realistic. Instead, we will add figures showing correlations between changes in climate variables and changes in land surface parameters, which is helpful in understanding the effects of land surface parameters on climate changes.

- The uncertainties in background albedo values (L. 527-558)
We will add the climate impacts of uncertainties in background albedo in the discussion part of the manuscript. The uncertainties of background albedo values do not influence much on the surface albedo during snow-cover period because snow cover leads to a much higher increase of surface albedo.

- The local effects of peatland forestation area on maximum difference of net surface solar radiation (L. 503-525).
Our reasoning is as follows: The maximum difference in net surface solar radiation is caused by the advanced snow clearance day due to peatland forestation, when the differences of surface albedo are biggest between snow covered peatland and non-snow covered forest. This means that the maximum difference of surface albedo is mostly dependent on snow albedo. As snow albedo has a negatively linear correlation to forest ratio (Fig. 4 in the original manuscript), the maximum difference in net surface solar radiation could be roughly estimated according to the difference of forest ratio. This part will be added in discussion.

- The uncertainties in translating FNFI land cover information to a compatible form with REMO (L.220-224).
We cannot use REMO with too low resolution, e.g. 100 km, for this study because it will make us lose too much information about the dynamics of the local effects of land cover changes on climate. We translated the ten FNFI land cover classes to the standard GLCCD land cover classes through comparing the definitions of land cover classes and allocating appropriate surface parameter values. We agree that it would be good to use a set of land surface parameter values produced for Finnish conditions, but it would require complete and consistent data on each parameter. Unfortunately, at this moment it is beyond our ability.

Runs with systematically changed input data/parameter values would give a better understanding of the relative importance of different factors to the results. The results of simulations are discussed in terms of peatland forestation. However, the two FNFI measurements that are 80 years apart record also many other changes of forest cover apart of peatland drainage. I would like too see a discussion what other factors (e.g. stocking) may have affected the simulations.

AR: Yes, climate effects are also shown in summertime in the southeast of Finland where mixed forest decreased and coniferous forest increased. This will be discussed with the spatial correlations required in the reply for general comment 3 from reviewer #3. Our simulations are performed with two static land cover states, and not coupled with dynamic vegetation model. So, we do not have stocking changes of the same type of forest.

The paper is well written. I have marked to the MS (Supplement) some passages that could be improved as well some other small comments.

Specific comments (in supplement: http://www.biogeosciences-discuss.net/11/C4600/2014/bgd-11-C4600-2014-supplement.pdf):

(1) Line 79-80: Is this for peatlands or in general?

AR: This refers to the averaged temperature changes over southern and northern Finland in general. This part will be modified to make it more clear to readers.

(2) Line 134 : This is unclear: do you consider the change of vegetation (e. g. forest growth) during the 18-year simulation? If this the case the growth factor should be explained in a detailed manner.

AR: The growth factor in REMO land surface scheme only describes the intra-annual cycles. Our simulations are static modeling based on two land cover maps. The definition of growth factor in the manuscript will be modified to be for clarity: the factor determines the seasonal growth characteristics of vegetation.

(3) Line 152: This is a bit unclear: later on Line 170-174 you explain that CORINE land cover map is used.

AR: GLCCD is the default land cover map to represent present land cover surface in REMO as mentioned in the manuscript. The subgrid-scale heterogeneity resolution of the improved hydrology scheme of REMO was set based on the standard land cover map (Hagemann and Gates, 2003). That work is independent to implementation of CORINE land cover map in REMO (Gao et al., 2014).

(4) Line 170: Earlier you say that there are 9.7 Mha peatlands.

AR: 9.7 million ha was the total peatland area of Finland in 1950s in Ilvessalo (1956). 22377 km^2 (7.4%) is the area of naturally treeless or sparsely treed peatland in the 10th FNFI (2000s). They are different.

(5) Line 178-179: So you mean in this paragraph that the spatial resolution (or the units are) is the same as in CLC but contents have been taken from FNFI? Maybe this paragraph is a bit difficult to follow.

AR: FNFI maps are in 3km resolution, where as CLC map is in 1km resolution. In the earlier study (Gao et al., 2014), CLC map is used instead of the standard GLCCD map to represent present land cover conditions for our model domain. In this study, we used both historic (1st) and present (10th) FNFI maps to describe the land cover changes in Finland, for consistency in land cover classification and spatial resolution. Therefore, CLC is substituted by FNFI10 to represent present land cover situation. All the land surface parameters allocated according to land cover maps are aggregated to 18 km resolution in REMO simulation.

(6) Line 200-223: This paragraph is difficult to follow. I suggest presenting the information (percentages) as table.

AR: This part of information has been presented as table 1. An introduction sentence will be added for Table 1 in the revised manuscript.

(7) Line 223-226: I do not understand what you are trying to say here.

AR: We are trying to explain the uncertainties of land cover changes in the selected subregions. To make it more clear, we will modify the original text as follows.

" One should notice that some uncertainties may arise from sampling in the FNFI1 and FNFI10 data. This applies especially for FNFI1, where the distance between inventory lines was as high as 26 km. Therefore, subregions that are smaller than 100 km × 100 km may not be sufficient to represent the actual land cover changes spatially. However, the dynamics of the local effects of land cover changes on climate cannot be detected when averaging climate signals over large areas with diverse land cover changes. Therefore, small subregions, which cover a range of land cover change intensities, are chosen to reflect local climate impacts due to different land cover changes."

(8) Line 282-283: This relationship requires a better explanation: either from physical principles or references to work, in which it was developed.

AR: Kotlarski (2007) is given as a reference for the linear relationship in snow albedo scheme in this paragraph. We found the last sentence of this paragraph is redundant with the sentence with Kotlarski (2007) as a reference in the above. We will delete this sentence.

(9) Line 288: Why this is the reason for 6 km resolution?

AR: The resolution of subgrid-scale heterogeneity adopted for the improved soil hydrology scheme (Hagemann and Gates, 2003) is set to be 10 times higher than the model resolution by using the default GLCCD. This is the context for setting the resolution of subgrid-scale heterogeneity in this study to be 3 times (18 km/3=6 km) higher than the model resolution (18 km), because the resolution of FNFI maps are 3 times lower than GLCCD.

(10) Line 298: add some words about calculation of dynamics of snow cover. It is an important model component in relation to the main result.

AR: We agree that the dynamics of snow cover is an important factor. The dynamics of snow dynamics in REMO is well described in Kotlarski (2007), therefore we will suggest that interested readers to refer to Kotlarski (2007) on the dynamics of snow cover.

(11) Line 447: Put this in caption of Fig. 10.

AR: Yes. It will be changed according to this suggestion.

(12) Line 495: Do you mean that REMO predicts winter time temperatures with bias?

AR: Yes. The cold bias over this model domain in wintertime simulated by REMO has been shown in Gao et al. (2014). The content of this paragraph will be changed according to general comment 1 from Reviewer #3.

(13) Line 503-525: You could test this by a simulation, in which you make this kind of change for the whole subregion1 (or all regions). I do not understand why this "Only around 20% ..." constitutes an explanation for differences in max. differences – the 20% change is also in the observations. Could it be that there are factors involved in max. observed differences that your simulations do consider?

AR: Indeed, the original text could be misunderstood. About 20% of subregion1 is changed due to peatland forestation (Table 1), whereas the observational data is measured at sites with open peatland and with forests. We have clarified this paragraph as follows.

"Furthermore, regional averaged difference in the simulated 11 day running mean net surface solar radiation of subregion1 (Fig. 5, d in the revised manuscript) agrees well with the observed differences in daily mean (1971-2000) net surface solar radiation (Fig. 4 in Lohila et al., (2010)) between open peatland and forest sites located in southern and northern Finland. The maximum differences in the observed net surface solar radiation at nutrient-rich sites are 40-45 W/m^2 (on DOY 70) in the south, and 80-90 W/m^2 (on DOY 110) in the north of Finland. At nutrient-poor sites, the maximum differences are 30-40 W/m^2(on DOY 80) in the south, and 60-70 W/m^2 (on DOY 115-120) in the north of Finland. The maximum difference in the simulated 11 day running mean net surface solar radiation averaged over subregion1 is 6.5 W/m^2 (on DOY 107). The timing of the maximum difference in our simulated results, for subregion1, falls within the range of that in the observed data. The much smaller magnitude of the maximum difference in the simulated results could be explained by the fact that only around 20% of the land was transformed from peatland to forests in subregion1. The maximum difference in net surface solar

radiation is caused by the advanced snow clearance day due to peatland forestation. The differences in surface albedo is biggest between snow covered peatland surface and non-snow covered forest surface, i.e. the maximum difference of surface albedo is mostly dependent on snow albedo. Snow albedo has a negative linear correlation with forest ratio (Fig. 4 in the original manuscript). Assuming that the entire land of subregion1 would have been changed from peatland to forests, the maximum difference in net surface solar radiation could be estimated to be five times larger, i.e. 32.5 W/m^2, which is within the range of observations."

Response to Anonymous Referee #2

General comments:

The authors provide an analysis on the biogeophysical effects of the dominant land cover change on regional climate in Finland. They found a spring warming due to the conversation of peatlands to coniferous forests that can be mostly related to the modification of the corresponding albedo values. The slight cooling in the growing season is explained with the increased evapotranspiration. The spatial distribution of the climate impacts are introduced for the whole country, furthermore the local scale effects are investigated more in detail for 5 selected subregions.

It is a very recent and important topic, with several practical aspects, especially regarding to the projected climate change and land cover change. The concepts of the manuscript are understandable, the results are interpreted correctly. The novelty of the presented work as well as the need of the regional scale and the use of a regional climate model is clearly explained.

The abstract of the discussion paper provide a concise summary of the paper but I would suggest referring to the practical application also in this place.

AR: We will add descriptions of practical application at the end of abstract as follows.

"The results from this study can be further integrally analysed together with biogeochemical effects of peatland forestation to provide background information for adapting future forest management to climate change mitigation. Moreover, they provide insights about the impacts of projected forestation of tundra in high latitudes due to climate change."

The Methodology chapter contains a very detailed and complete introduction and evaluation of the applied land cover maps and the land surface scheme and parameterization of the regional climate model. It underlines the importance of the appropriate representation of the land cover in climate models that has been improved by the corresponding author. I suggest keeping sect. 2 shorter and including the technical details in the Appendix.

AR: We will move Section 2.3 (Modifications in REMO LSS in this study) to Appendix.

The uncertainties and the limitations of the applied methods are well discussed at the end of the work.

Specific comments:

Following are few comments and questions that the authors should consider clarifying:

(1) The simulated changes of temperature, evapotranspiration, . . . and their magnitude are closely related to the modification of the corresponding main land surface parameters in the climate model. Therefore for the better representation and interpretation of the process chain, I would suggest to include some maps about the changes (2000s vs. 1920s) of albedo, leaf area index and fractional vegetation cover for the whole domain (e.g. on monthly timescale, next to figure 3).

AR: We agree that to show the monthly changes in land surface parameters together with the changes in climate variables is helpful for representation and interpretation of the process chain. For this purpose, we adopted the approach suggested by reviewer #3 in general comment 3 to show correlation relationships. Moreover, we want to keep the length of the manuscript not too long as suggested by Reviewer #3 in general comment 1 to cut down the number of figures. Therefore, please refer to the response to general comment 3 of Reviewer #3 about this comment.

(2) In order to support the better understanding of the main outcome and to make possible to compare the results of the 5 subregions, please add a summary-table that includes the modification of the land cover types (in %), the corresponding change of the albedo, leaf area index and fractional vegetation cover as well as the impacts on the analysed climatic variables for each subregions (complete table 1 with the above mentioned information).

AR: The impacts on analyzed climatic variables for each subregion with daily time resolution have been shown in Fig. 8 in the original manuscript. The change of surface parameters of five subregions for the most interesting periods will be shown in the correlation figures as mentioned in the above specific comment 1. Thus, we believe that there is no longer necessary to add this table anymore.

(3) I would suggest preparing a sensitivity study with unchanged vegetation cover for the same time periods. In this way the contribution of the GHG emission and land cover change to the observed climate tendency could be separately assessed.

AR: The two simulations in this study were conducted over the same time period (1979.1.1 - 1996.12.31) with two different land cover maps. ERA-interim is used as our boundary forcing data. The GHG concentrations for the two simulations are the same. Therefore, the impacts on climate conditions are only from the changes in land cover.

To estimate the contributions of increased GHG concentrations to the observed climate tendency, we cannot simply use our boundary forcing data over the same time period to do the simulations with two levels of GHG concentrations. It is because that ERA-interim reanalysis data is based on observational data. For complete consideration, a global model is needed. Additionally, in response to the general comment 1 from Reviewer #3, the trend maps for monthly mean daily maximum temperature and daily minimum temperature are investigated for March and April. We consider that the trend of daily maximum temperature is influenced by albedo-mediated temperature changes locally, while the trend of daily minimum temperature is more closely related to general climate change caused by global GHGs increases. The local effects in the trends of daily maximum temperature suggest that our modeled results show qualitatively a good correspondence to observational data.

(4) Outlook: How does projected climate change affect the existing land cover (primarily forests and peatlands) in Finland? How could these changes alter the regional climate?

AR: The land cover in Finland is strongly managed. Therefore, we will generally discuss the potential land cover change under the projected climate for high latitudes, and its influence on climate. The content below will be added in discussion part.

"The biogeophysical impacts of vegetation-climate feedbacks on climate are modest in comparion to the effects of increased GHGs for Europe, but local, regional and seasonal effects can be significant (Wramneby et al., 2010). However, studies with dynamic vegetation models under climate projections with increased GHGs indicate that more carbon will be gained to terrestrial ecosystems in high-latitudes by the end of this century (Fallon et al., 2012; Zhang et al., 2014). This is due to increase in woody plants that induce biogeophysical feedbacks with an earlier onset of growing season."

(5) Please refer short in the discussion part also to the possible biogeochemical feedbacks: how are the carbon sequestration and methane concentrations altered by the forest cover increase/peatland decrease? What are the climatic impacts of these changes?

AR: The discussion about biogeochemical aspects will be added as follows.

"Peatland is a significant source of CH_4 emissions, and the amount of CH_4 emission is sensitive to temperature, water table level, plant root depth and soil nutriention level, etc. (Melton et al. 2013; Turetsky et al., 2014; Lohila et al., 2010). After peatland forestation, the soil water table level goes down leading to increased CO_2 release at the expense of CH_4 release (Minkkinen and Laine, 2006). As time goes by, carbon sequestration by the tree growth and the formation of a new litter layer could compensate the carbon loss from peatland. Lohila et al. (2010) combined the radiative forcing effects from the differences of albedo and GHG fluxes due to peatland forestation at site-level, and showed net cooling at two soil nutrient-rich sites in the south and north and one soil nutrient-poor site in the south of Finland. Accounting for such local impacts in a regional climate model requires very sophisticated process descriptions and detailed parameterisation of soil properties."

Please also note the supplement to this comment: http://www.biogeosciences-discuss.net/11/C4689/2014/bgd-11-C4689-2014- supplement.pdf

Specific comments (in supplement):

(1) Page 11253, Line 5: Suggestion: keep shorter sect. 2.1, 2.2 and 2.3, and include the technical details in an Appendix.

AR: Answered in the response to general comments.

(2) Page 11256, Line 2: Where exactly? Figure 2 should be mentioned here.

AR: Fig. 2 is mentioned in the following sentence for the regional differences, where the total fractional changes over Finland is shown.

(3) Page 11263, Line 14: This kind of information is hard to follow in this form (i.e. long paragraphs), please add a table that summarizes the main outcome for the 5 regions.

AR: Answered in specific comment 2.

(4) Page 11265, Line 23: Please show the corresponding LAI and fractional vegetation cover changes on figures for the whole domain.

AR: Answered in specific comment 1.

(5) Page 11266, Line 19: It would be interesting to have some information on the effect of the GHG concentration increase on the observed temperature tendency (i. e. without any land cover change)

AR: Answered in specific comment 3.

(6) Page 11288, Figure 8: the ET values with negative signs are confusing.

AR: Agreed. ET values in Fig. 8 will be changed to be with normal signs.

Response to Anonymous Referee #3

General comments:

Gao and co-workers mainly analysed the climate effects of peatland afforestation as simulated by REMO. As an experimental set-up they used the land cover in 1920s and compared it against the land cover in the 2000s and compare 5 subregions with contrasting land cover changes. Although the manuscript is already in good shape, its potential impact is likely to further increase by implementing the following general suggestions:

(1) A more careful selection of the figures could reduce the length of the manuscript and better distinguish the details from the main messages. Fig 5 and Fig 6 could be display with fewer months. That would allow plotting larger subplots without loosing information. Figure 6 is barely mentioned in the manuscript, the patterns are correctly described by random. The figures add little information.

AR: Agreed. Fig. 5 in the original manuscript will be only shown with spring and summer months, and autumn and winter months will be excluded. Fig. 6 in the original manuscript will not be shown in the revised manuscript. The excluded figures will be submitted as supplements.

The information contained in fig 1 could easily be added to any of the subsequent figures (or better repeated on all subsequent maps). Fig 1 shows the altitude of the sites but nothing is done with that information.

AR: We consider Fig. 1 should be kept because it is the only figure in the manuscript that shows the entire model domain, and orography is an important factor for regional climate. However, we will revise Fig. 1 with a more proper color bar to show the orography, and we will also add the relaxation zone used in REMO simulations for this domain (Please see the *revised Fig. 1 below).*

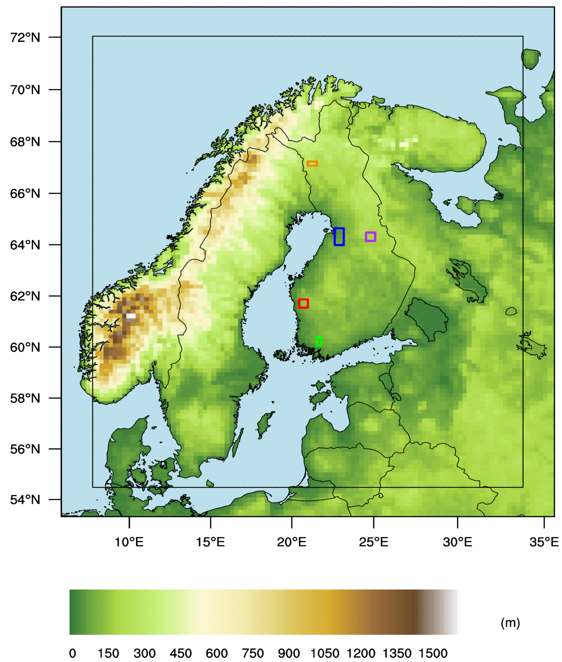

Fig. 1 Orography of the model domain, and the five selected subregions (subregion1 – blue; subregion2 – red; subregion3 – purple; subregion4 – green; subregion5 - orange). The inner black frame shows the extent of the relaxation zone, i.e. the eight outer most gridboxes in each direction.

The information in Fig 3 could be added to Table 3.

AR: Agreed. This information will be added to Table 3 in two additional columns.

In its current presentation, figure 11 does not help to convince that the model does a good job. I suggest a correlation graph between the modelled and observed temperature changes in February, March and April would better present the message.

AR: Agreed. However, we found that the spatial correlations between modeled and observed temperature changes could not help us in this problem. To address this, we investigated the temperature trends over 40 years (1959-1998) for March and April based on monthly mean daily maximum and daily minimum temperatures from E-OBS gridded observational dataset in 0.25 degree resolution. We consider that the trend of daily maximum temperature is influenced by albedo-mediated temperature changes locally for March and April, while the trend of daily minimum temperature is more related to the general climate change caused by global GHGs increases. The local effects in the trends of daily maximum temperature suggest that our modeled results show qualitatively a good correspondence to observational data. The major areas of peatland forestation, subregion1 and subregion2, are highlighted and statistically significant in the trends of maximum temperatures in both March and April but not shown in the trend of minimum temperature. The new temperatrue trend maps are shown below.

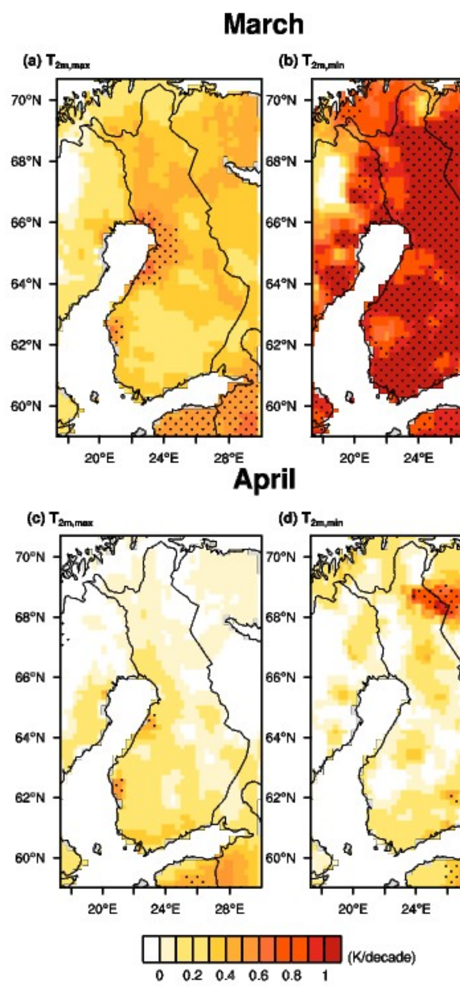

Fig.2 Temperature trends over 40 years (1959-1998) for (a, c) monthly mean daily maximum and (b, d) monthly mean daily minimum temperatures of March and April. The areas covered with black dots are statistical significant ($p<0.1$).

(2) The manuscript deals with the effect of land cover change and one of its strengths, i.e., that it has also an area of

peatland restoration, is hardly used. Subregions 1 and 2 are discussed in detail much fewer attention is given to subregion5 but this could add a very interesting perspective to the discussion.

AR: We cannot really say subregion5 as a peatland restoration area because the land cover change of subregion5 is an artificial effect due to the uncertainties in FNFI maps (discussed in Section 2.2). However, we included subregion5 in the analysis because it is interesting to see the modeled climate effects of this area that with decreased forests and increased peatland. Thus, we chose subregion5 as a comparison to subregion1 and subregion2 where the land cover change actually took place, with less attention given to subregion5 .

(3) There is no figure showing the relationship between land cover change and climate change. Simple correlations between all land covers in table 1 and the observed temperature and precipitation differences may result in some interesting perspective(s). The same analysis could be repeated for the drivers, i.e., change in albedo, change in ET, …

AR: Agreed. We investigated the spatial correlations between the changes in the two surface energy balance relevant variables, surface albedo and ET, and T_{2m}. Consequently, the changes in surface albedo and ET are correlated to the changes in the surface parameter values which describe land cover changes. Monthly means of 15-year averaged changes of March and June are selected to represent springtime and summertime effects, respectively. The following plot and descriptions about those relationships will be added in the manuscript.

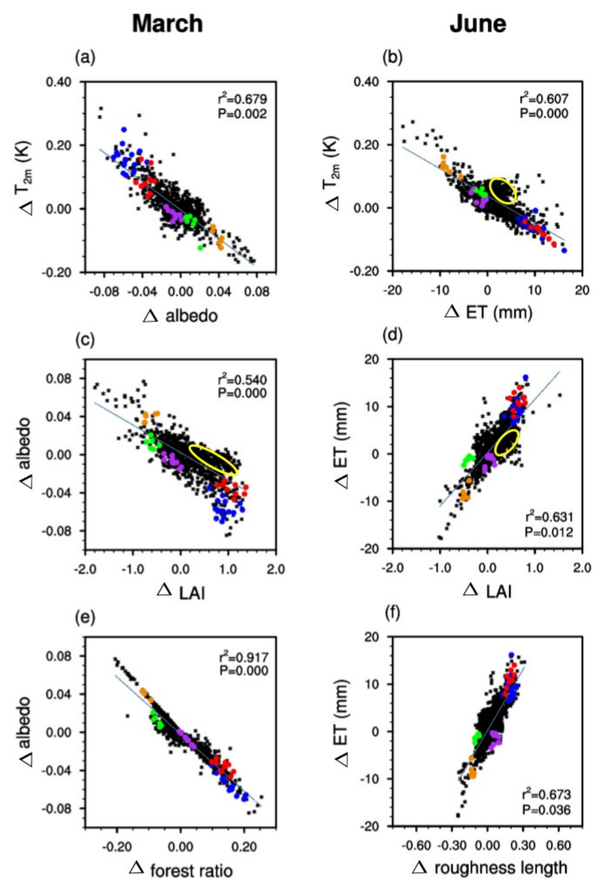

Fig. 3 Spatial correlations between (a) changes in monthly averaged daily mean two-metre air temperature (T_{2m}) and changes in albedo for March, (b) changes in T_{2m} and changes in ET for June, and also relationships between changes in land surface parameters in REMO LSS following land cover changes and changes in albedo (c, e) (changes in ET (d, f) in the corresponding month. The changes in the gridboxes in selected subregions are shown with coloured dots (subregion1--blue; subregion2--red; subregion3—purple; subregion4--green; subregion5--orange). The gridboxes in yellow circles show the changes in the southeast area of Finland.

"To assess the generality of the causal relationships between land cover changes and climate variables, the spatial correlations between changes in the two surface energy balance relevant variables, surface albedo and ET, and T_{2m} are

investigated. Consequently, the spactial correlations between changes in surface albedo and ET and changes in the surface parameter values are also explored. The correlations with green vegetation ratio is not shown in Fig. 3, because LAI and green vegetation ratio are both modulated with the monthly varying growth factor by the same scheme, and they are highly correlated (pearson correlation coefficient, r^2= 0.984 for March, r^2=0.674 for June). Monthly means of 15-year averaged changes in March and June are selected to represent springtime and summertime, respectively. The changes in T_{2m} are in accordance with the changes in surface albedo in March (Fig. 3, a), which is almost linearly correlated with the changes in LAI (Fig. 3, c) and forest ratio (Fig. 3, e). The T_{2m} changes in June are linearly correlated with ET changes over most of the area (Fig. 3, b). In general, the changes in ET are also correlated with the changes in LAI (Fig. 3, d), roughness length (Fig. 3, f) and forest ratio (yearly-constant, not shown), despite the influences from drought that may happen in late summer. Overall, the changes in surface albedo and ET are closely dependent on the changes in land surface parameters, which are induced by the changes in fractional coverages of land cover types in the five subregions (Table 1). The changes in T_{2m} are mainly modulated by the changes in albedo and ET in spring and summer, respectively. Some gridboxes located in the southeast of Finland, where mixed forest was substituted by coniferous forest mainly, show deviations in the correlations with LAI (marked by yellow circles in Fig. 3, b, c, d). In this area, LAI increased with almost no change in forest ratio, which lead to relatively smaller decrease in surface albedo compared to other areas with the same magnitude of changes in LAI in March; the ET-induced cooling is outweighted by the albedo-induced warming, which causes a slight warming effect in June. In the following summer months, July and August, the ET-induced cooling effect typically gets smaller because of surface water limitation and consequent warming."

(4) At several places in the results and discussion, cloud cover and atmospheric inversions are mentioned as drivers of some of the observed changes but no evidence is provided to the reader. Is this a result from the analysis or a (logical) induction by the authors.

AR: It is a logical induction according to the results shown in Fig. 8 (in the original manuscript). In autumn and winter, there are varied differences of temperature but no differences in net surface solar radiation. Also there are no differences in ET, as well as in latent heat flux. Thus, the differences of long wave radiation is the only factor affecting surface energy partition.

(5) In fig 8 subplots have different units. In the text these subplots are compared as if they have the same units (p11262, 20-22). Converting the units would result in a more convincing presentation.

AR: We found by showing percentage changes for those variables are not helpful to illustrate the results. To make this part more clear, we will revise of the text as follows.

"T_{2m} of subregion1 shows a warming of 0.1 K to 0.2 K from February till the end of March, and an evident peak of increase from early April to early May (from DOY 95 to DOY 125), which reaches a maximum of 0.5 K in late April. T_{2m} of subregion2 has the same developement as subregion1 throughout the whole year, but the warming is much smaller and the biggest difference occurs in the beginning of April being only 0.12 K. This is consistent with the differences in snow depth. The snow-cover period in subregion2 is shorter along with an earlier maximum difference in snow depth. Moreover, those characteristics of the differences in snow depths are in agreement with the differences in surface albedo qualitatively because snow is the key factor that controls the surface albedo in the snow-cover period. From the beginning of May to the beginning of October, T_{2m} turns to show a cooling of less than 0.1 K in subregion1 and subregion2, because the cooling caused by ET exceeds the warming caused by the slightly lower albedo. The variability of the differences in net surface solar radiation in the growing season is induced by the variability of cloud cover rather than surface albedo. In November, December and January, the differences in T_{2m} vary in both directions. In high-latitudes, incoming solar radiation is quite small and cloud cover fraction is high in late autumn and winter. Therefore, the differences in surface albedo are not able to induce differences in net surface solar radiation in this period. Instead, the surface air temperature is sensitive to changes in the long-wave radiation balance that may lead to atmospheric air temperature inversion under a clear sky, manifesting itself as extreme cold surface air temperature. Thus, the variability of the differences in cloud cover caused by short-term variations in the climate contributes to varied differences in T_{2m} in this period."

Specific comments:

(1) The term 'unproductive peatland' contains some contradiction as these sites are so fertile that they are drained and used for forestry and agriculture. What is the reference for the word 'unproductive'? Euro's, water, carbon, . . .?

AR: Unproductive land in Finnish National Forest Inventory is defined as naturally treeless land or land has the potential capacity to produce a mean annual increment of less than 0.10 m^3/ha of stem wood over bark, which can be referred to Tomppo et al. (2011). Thus, unproductive peatland means naturally treeless or sparsely treed peatland. On unproductive *peatland, the growth limiting factor is not site infertility, but excess of water. Therefore, peatlands were drained to stimulate forests growth in Finland in the past. To make it more clear, the term 'unproductive peatland' will be changed to 'naturally treeless or sparsely treed peatland' in the manuscript.*

(2) The objectives (top page 11253) are rather vague.

AR: Agreed. We will modify it as: The intention of this study is to understand how peatland forestation that took place in Finland influences regional climate conditions from biogeophysical aspects.

(3) Reword and add some details. Mention the effects on keeping land cover unchanged outside of Finland. This basically means that your experiment can quantify the impact of land cover change for Finnish climate but is not suitable to attribute observed changes in climate to land cover change.

AR: Agreed. We will add the discussion below about this point in the part that compares simulated results with observational data.

"However, it is difficult to compare the exact magnitudes and patterns of temperature changes because observational data contains contributions from other factors, for instance, the effects of climatic teleconnections from land cover changes in surrounding areas of Finland and short lived climate forces, such as aerosols and reactive trace gases (Pitman et al. 2009)."

References:

Falloon, P. D., Dankers, R., Betts, R. A., Jones, C. D., Booth, B. B. B., and Lambert, F. H.: Role of vegetation change in future climate under the A1B scenario and a climate stabilisation scenario, using the HadCM3C Earth system model, Biogeosciences, 9, 4739-4756, 2012.

Gao, Y., Weiher, S., Markkanen, T., Pietikäinen, J.-P., Gregow, H., Henttonen, H. M., Jacob, D.,and Laaksonen, A.: Implementation of the CORINE land use classification in the regional climate model REMO, Boreal Environ. Res., accepted, 2014.

Lohila, A., Minkkinen, K., Laine, J., Savolainen, I., Tuovinen, J.-P., Korhonen, L., Laurila, T., Tietäväinen, H., and Laaksonen, A.: Forestation of boreal peatlands: impacts of changing albedo and greenhouse gas fluxes on radiative forcing, J. Geophys. Res.-Biogeo., 115, G04011, doi:10.1029/2010JG001327, 2010.

Melton, J. R., Wania, R., Hodson, E. L., Poulter, B., Ringeval, B., Spahni, R., Bohn, T., Avis, C. A., Beerling, D. J., Chen, G., Eliseev, A. V., Denisov, S. N., Hopcroft, P. O., Lettenmaier, D. P., Riley, W. J., Singarayer, J. S., Subin, Z. M., Tian, H., Zürcher, S., Brovkin, V., van Bodegom, P. M., Kleinen, T., Yu, Z. C., and Kaplan, J. O.: Present state of global wetland extent and wetland methane modelling: conclusions from a model inter-comparison project (WETCHIMP), Biogeosciences, 10, 753-788, doi:10.5194/bg-10-753-2013, 2013.

Minkkinen, K. and Laine, J.: Vegetation heterogeneity and ditches create spatial variability in methane fluxes from peatlands drained for forestry, Plant and Soil, 285, 289-304, doi: 10.1007/s11104-006-9016-4, 2006.

Pitman, A. J., de Noblet-Ducoudré, N., Cruz, F. T., Davin, E. L., Bonan, G. B., Brovkin, V., Claussen, M., Delire, C., Ganzeveld, L., Gayler, V., van den Hurk, B. J. J. M., Lawrence, P. J., van der Molen, M. K., Müller, C., Reick, C. H., Seneviratne, S. I., Strengers, B. J., and Voldoire, A.: Uncertainties in climate responses to past land cover change: First results from the LUCID intercomparison study, Geophysical Research Letters, 36, L14814, doi: 10.1029/2009GL039076, 2009.

Tomppo, E., Heikkinen, J., Henttonen, H. M., Ihalainen, A., Katila, M., Mäkelä, H., Tuomainen, H., and Vainikainen, N.: Designing and Conducting a Forest Inventory-case: 9th National Forest Inventory of Finland, Springer, The Netherlands, 2011.

Turetsky, M. R., Kotowska, A., Bubier, J., Dise, N. B., Crill, P., Hornibrook, E. R. C., Minkkinen, K., Moore, T. R., Myers-Smith, I. H., Nykänen, H., Olefeldt, D., Rinne, J., Saarnio, S., Shurpali, N., Tuittila, E.-S., Waddington, J. M., White, J. R., Wickland, K. P. and Wilmking, M.: A synthesis of methane emissions from 71 northern, temperate, and subtropical wetlands, Global change biology, 20, 2183-2197, doi: 10.1111/gcb.12580, 2014.

Wramneby, A., Smith, B., and Samuelsson, P.: Hot spots of vegetation-climate feedbacks under future greenhouse forcing in Europe, Journal of Geophysical Research – Atmospheres, 115, D21119, doi:10.1029/2010JD014307, 2010.

Zhang, W., Jansson, C., Miller, P. A., Smith, B., and Samuelsson, P.: Biogeophysical feedbacks enhance Arctic terrestrial carbon sink in regional Earth system dynamics, Biogeosciences, 11, 5503-5519, doi:10.5149/bg-11-5503-2014, 2014.

Manuscript prepared for Biogeosciences Discuss.
with version 2014/07/29 7.12 Copernicus papers of the LaTeX class copernicus.cls.
Date: 10 November 2014

Biogeophysical impacts of peatland forestation on regional climate changes in Finland

Y. Gao[1,2], T. Markkanen[1], L. Backman[1], H. M. Henttonen[3], J.-P. Pietikäinen[1], H. M. Mäkelä[1], and A. Laaksonen[1,4]

[1]Finnish Meteorological Institute, P.O. Box 503, 00101 Helsinki, Finland
[2]University of Helsinki, Department of Physics, P.O. Box 64, 00014 Helsinki, Finland
[3]Finnish Forest Research Institute, P.O. Box 18, 01301 Vantaa, Finland
[4]University of Eastern Finland, Department of Applied Physics, P.O. Box 1627, 70211 Kuopio, Finland

Correspondence to: Y. Gao (yao.gao@fmi.fi)

Abstract

Land cover changes can impact the climate by influencing the surface energy and water balance. Naturally treeless or sparsely treed peatlands were extensively drained to stimulate forest growth in Finland over the second half of 20th century. The aim of this study is to investigate the biogeophysical effects of peatland forestation on regional climate in Finland. Two sets of 18-year climate simulations were done with the regional climate model REMO by using land cover data based on pre-drainage (1920s) and post-drainage (2000s) Finnish National Forest Inventories. In the most intensive peatland forestation area, located in the middle west of Finland, the results show a warming in April of up to 0.43 K in monthly averaged daily mean two-metre air temperature, whereas a slight cooling of less than 0.1 K in general is found from May till October. Consequently, snow clearance days over that area are advanced up to 5 days in the mean of 15 years. No clear signal is found for precipitation. Through analysing the simulated temperature and energy balance terms, as well as snow depth over five selected subregions, a positive feedback induced by peatland forestation is found between decreased surface albedo and increased surface air temperature in the snow melting period. Our modelled results show good qualitative agreements with the observational data. In general, decreased surface albedo in snow-melting period and increased evapotranspiration in the growing period are the most important biogeophysical aspects induced by peatland forestation that cause changes in climate. The results from this study can be further integrally analysed with biogeochemical effects of peatland forestation to provide background information for adapting future forest management to mitigate climate warming effects. Moreover, they provide insights about the impacts of projected forestation of tundra in high latitudes due to climate change.

1 Introduction

Climate response to anthropogenic land cover change happens more locally and occurs on a much shorter time scale, compared to global warming due to increased greenhouse gases (IPCC, 2013). The influences on the climate from the biogeophysical effects caused by land cover changes can enhance or reduce the projected climate change (Bathiany et al., 2010; Bonan, 2008; Feddema et al., 2005; Gálos et al., 2011; Göttel et al., 2008; Ge and Zou, 2013; Pielke et al., 2011, 1998; Pitman, 2003). Especially for the climate impacts of past large-scale afforestation, studies show that the most obvious effects from the increase of forests in boreal areas are warming during snow-cover periods, due to decreased surface albedo, and cooling in summertime from increased evapotranspiration (ET) in tropical areas with sufficient soil moisture (Bala et al., 2007; Betts, 2000; Betts et al., 2007).

Vast areas of naturally treeless or sparsely treed peatlands have been drained to grow forests for timber production in northern European countries (Päivänen and Hånell, 2012). In Finland, it is the dominant land cover change over the last half century, due to the high fraction of pristine peatland and the needs for timber production. The total peatland area of Finland was estimated to be 9.7 million ha in the 1950s (Ilvessalo, 1956). In the beginning of 2000s, the area of drained peatland for forestry was estimated to be 5.7 million ha by Minkkinen et al. (2002) and 5.5 million ha by Tomppo et al. (2011). The area of drained peatlands is unlikely to increase further because no more public subsidisation is given for the first-time drainage of peatlands, along with the increased awareness of natural conservation (Metsätalouden kehittämiskeskus Tapio, 1997). The area of restored mires was 15 000 ha between 1990 and 2008 (www.biodiversity.fi/en/indicators/mires/mi17-mire-restoration) (Kaakinen and Salminen, 2006). However, land cover change is not only a result of human land-use activities but can also be a consequence of climate change. Global warming in the future is also considered to be a factor that affects boreal peatland through water-level drawdown due to increased ET (Laiho et al., 2003; Laine et al., 1995).

Attention has been paid to the climate effects of peatland forestation. A decrease in the local night-time minimum temperature during the growing season was observed roughly for the first 15 years after drainage (Solantie, 1994). The reason for this nocturnal cooling phenomenon is the insulation of lower soil layers from the atmosphere by dry peat. Therefore, the heat flux from drained peat soil can not compensate for the radiative cooling at the surface, which leads to a drop in daily minimum temperature (Venäläinen et al., 1999). On a longer time scale, the growing forest on formerly open peatlands leads to a decrease in surface albedo. The reasons for this are the darker tree-cover in comparison to the lighter moss/grass-cover in the snow-free period, and the partial snow cover in forest areas compared to the full snow cover in open area in snow-cover period. This increases the daily maximum temperature due to an increase in the absorption of shortwave radiation (Solantie, 1994). Consistent results on the seasonal cycles of surface albedo and net surface solar radiation due to peatland forestation were found by Lohila et al. (2010) based on measurement data at two pairs of drained and undrained peatland sites located in the south and north of Finland, showing a notable decreased surface albedo and corresponding increased net surface solar radiation in springtime. Furthermore, Lohila et al. (2010) indicated the local climate impacts of peatland forestation by investigating long-term (1961–2008) spring surface temperature trends over southern ($< 65°$ N) and northern ($> 65°$ N) Finland. The largest positive day-time maximum temperature trend of 0.64 K decade^{-1} happened in April in southern Finland, where a total of 2.7 million ha of peatlands were drained (Hökkä et al., 2002). The night-time minimum temperature trend through the same period was 0.37 K decade^{-1}. Lohila et al. (2010) attributed the substaintially larger increase in the day-time maximum temperature than in the night-time minimum temperature to the change in surface radiative properties after drainage.

However, these studies about the effects of peatland forestation on climate are based on site-level data or observation based regional data, which can not attribute the climate impacts to different influencing factors. Specifically, they can not distinguish the local biogeophysical effects from the global climate change due to the increase of GHG concentrations. The climate effects of peatland forestation have not been quantified on a regional scale/country level by particularly investigating the biogeophysical effects. Also, the magnitude and pattern of land-use change effects on climate depends on the regional conditions, for instance soil property, topography and so on. Information from regional studies is essential for the development of future strategies for climate mitigation or forest management. Thus, it is necessary to investigate the effects regionally and systematically.

In recent years, regional climate models have become suitable for simulating regional climate in a fine resolution to resolve small-scale atmospheric circulation (Déqué et al., 2005; Jacob et al., 2007, 2001; McGregor, 1997). For this, a regional climate model with a realistic land scheme to interpret more detailed land surface information needs to be applied.

In this study, the long-term climate effects caused by peatland forestation are assessed from two sets of 15- year simulation results with the regional climate model REMO, by using the historical (1920s) and present-day (2000s) land cover conditions, respectively. The intention of this study is to understand how peatland forestation that took place in Finland influences regional climate conditions from biogeophysical aspects.

2 Model description and methodology

2.1 REMO climate model

The regional climate model REMO is a three-dimensional hydrostatic atmospheric circulation model developed at Max Planck Institute, Germany (Jacob et al., 2007, 2001; Jacob and Podzun, 1997). Its dynamical core is based on the "Europamodell", the former numerical weather prediction model of German Weather Service (Majewski, 1991). The land surface scheme (LSS) of REMO mainly follows that of the global atmosphere circulation model ECHAM4 (Roeckner et al., 1996), with several physical package updates (details are shown below). The prognostic variables are pressure, temperature, horizontal wind components, specific humidity, cloud liquid water and ice. REMO is driven by large-scale forcing data according to the relaxation scheme (Davies, 1976). The eight outer most gridboxes at each lateral boundary are the sponge zone.

Because land cover is central for this study, a brief introduction of the LSS in REMO is given below. In REMO LSS, the total area of each model grid box is composed of fractions of land (vegetation cover and bare soil), water (ocean surface and inland lake) and sea ice (Semmler et al., 2004). The biogeophysical characteristics of major land cover classes

(Olson, 1994a, b) are described by the following surface parameters: background surface albedo (albedo over snow-free land areas), roughness length, fractional green vegetation cover, leaf area index (LAI; one-sided green leaf area per unit ground area), forest ratio (fr; fractional coverage of trees regardless of their photosynthetic activity), soil water holding capacity (maximum amount of water that plants may extract from the soil before wilting begins) and volumetric wilting point (percentage of moisture in a soil column below which plants start to wilt) (Hagemann, 2002; Hagemann et al., 1999). The land surface parameters are averaged linearly according to fractional coverage of land cover types within a model gridbox, except for the roughness length that is averaged logarithmically (Claussen et al., 1994; Hagemann et al., 1999). As LAI, fractional green vegetation cover and background surface albedo strongly depend on the vegetation phenology, they are prescribed with intra-annual cycles by using a monthly varying growth factor that determines the seasonal growth characteristics of the vegetation (Hagemann, 2002; Rechid and Jacob, 2006). The growth factor for latitudes higher than 40° North or South is derived from a two-metre temperature climatology (Legates and Willmott, 1990), in other latitudes the fraction of photosynthetically active radiation is used.

The simple bucket scheme (Manabe, 1969) is used for soil hydrology where the partitioning of surface runoff and infiltration follows the Arno-Scheme (Dumenil and Todini, 1992). The soil temperature profile from the ground surface to around 10 m deep is described by five soil layers with increasing thickness. The heat conductivity and heat capacity, in the heat conduction equation for calculating the soil temperature, depend on the soil types (Kotlarski, 2007). The distribution of soil types is from FAO/UNESCO soil map of the world (FAO/UNESCO, 1971–1981; Kotlarski, 2007).

The Arno-Scheme used for the soil hydrology was further improved by considering the high resolution subgrid-scale heterogeneity of the field capacities within a climate model gridbox (Hagemann and Gates, 2003). The resolution of subgrid-scale heterogeneity is set to be 10 times higher than the resolution of the model by using the default REMO land cover map–Global Land Cover Characteristics Database (GLCCD) (Loveland et al., 2000; US Geological Survey, 2001). The three parameters in the improved Arno-Scheme are accounting for the shape of the subgrid distribution of soil water capacities (Beta), subgrid minimum (W_{min}) and maximum (W_{max}) soil water capacities. Also, the original annual background albedo cycle was modified by using MODIS satellite data between 2001 and 2004 in order to derive more realistic global distributions of pure soil albedo and pure vegetation albedo, which are then used to compute the annual background albedo cycle with monthly varying LAI (Rechid, 2008; Rechid et al., 2009).

2.2 The model domain and land cover data sets

Our model domain covers Fennoscandia, a part of Russia and the northern part of Central Europe, and it is centred on Finland (Fig. 1). Typical features influencing the climate of this domain include: the North Atlantic Ocean and the Baltic Sea that surround the Fennoscandian countries; many inland lakes located in Sweden and Finland; the relatively high Scandinavian mountain range; while the rest of the area has a topography lower than 300 m above sea level.

The default land cover map in REMO is GLCCD. However, its description of the land cover in Finland is unrealistic. For instance, there is no peatland in Finland in GLCCD, whereas 7.4 % (22 377 km^2) of the land is covered by naturally treeless or sparsely treed peatlands in the 10th Finnish National Forest Inventory (FNFI10) (Korhonen et al., 2013). GLCCD was therefore substituted by the more realistic and up-to-date CORINE land cover map (CLC; 2006) for the same model domain in Gao et al. (2014), except for the Russian part where CLC (2006) is not available. Unfortunately, land cover maps describing land cover conditions of Finland before the most intensive period of peatland drainage in the 1960s are quite limited. Nevertheless, the data collected in the 1st Finnish National Forest Inventory (FNFI1) provide the possibility for tracing back the land cover condition of Finland in the 1920s (Ilvessalo, 1927; Tomppo et al., 2010). Also, the FNFI10 is adopted to describe the land cover condition of Finland in 2000s instead of CLC (2006), with the aim to avoid the uncertainties in comparing land cover maps with different land cover classification methods and different spatial resolutions. The FNFI1 and FNFI10 land cover maps are post-products that were specially prepared for this study from the respective FNFI field measurement data.

The detailed description of the procedures for deriving the FNFI1 and FNFI10 land cover maps is shown in Appendix A. The two FNFI land cover maps are in 3 km resolution and include ten land cover classes following CLC-nomenclature.

The fractional coverage for the ten land cover classes over the land area of Finland in the 1920s and the changes from the 1920s to the 2000s based on the two FNFI land cover maps are shown below (fractional coverage in the 1920s; changes from the 1920s to the 2000s): Coniferous Forest (33.0 %; 5.2 %); Mixed Forest (13.5 %; −5.7 %); Broad-leaved Forest (4.7 %; −0.8 %); Artificial Areas (0.7 %; 4.1 %); Natural Grasslands (3.4 %; −3.4 %); Peat Bogs (14.3 %; −5.2 %); Open Spaces (1.5 %; −0.1 %); Transitional Woodland/Shrub (18.9 %; 4.3 %); Moors and heathland (2.1 %; 0.7 %); and Agricultural Areas (8.0 %; 0.9 %). Regional differences of those land cover classes can be seen in Fig. 2. In the FNFI maps, the land cover class Peat Bogs is defined as naturally treeless peatland and pine mires where the stocking level is low or the mean height of trees is below 5 m at maturity. Therefore, the shifting from Peat Bogs to forests represents the major land cover change due to peatland forestation.

In addition to regional inspections, five subregions were selected to represent different land cover change conditions between FNFI1 and FNFI10 (Fig. 1), and the changes of fractional coverage of the ten land cover classes in those five subregions are given in Table 1. This was done to specifically assess the local climate effects of different intensities of peatland forestation. From subregion1 to subregion4, there is a decrease in the reduction of Peat Bogs. Subregion1 and subregion2 are two peatland forestation areas located in the middle and south of Finland, respectively. In subregion1 and subregion2, there were decreases in the fractional coverage of Peat Bogs of more than 20 %, and the decreases were mainly compensated by Coniferous Forest. The decrease in the fractional coverage of Peat Bogs was 2 % less in subregion2 than that in subregion1, but the increase in the fractional coverage of Coniferous Forest was 5 % higher in subregion2 than that in subregion1. The total increase in the fractional coverage of forest types was about 16 % in both subregion1 and subregion2. Subregion3 is located in the east of subregion1. There was a 12 % decrease in the fractional coverage of Peat Bogs, but instead of an increase of forests, the fractional coverage of Transitional Woodland/Shrub increased by 14.3 %. Subregion4 is an area where the most intensive anthropogenic activities have occurred in the five subregions. There was a 14 % decrease in the fractional coverage of forest types and a 3.8 % decrease in that of Peat Bogs, with a 5.7 % increase in the fractional coverage of Artificial Areas and a 10.5 % increase in that of Agriculture Areas. Subregion5 is an area with an 8.64 % increase in the fractional coverage of Peat Bogs and a 16.3 % decrease in the fractional coverage of forest types. Herein, one should notice that some uncertainties may arise from sampling in the FNFI1 and FNFI10 data. This applies especially for FNFI1, where the distance between inventory lines was as high as 26 km. Therefore, subregions that are smaller than $100\,\mathrm{km} \times 100\,\mathrm{km}$ may not be sufficient to represent the actual land cover changes spatially. However, the dynamics of the local effects of land cover changes on climate can not be detected when averaging climate signals over large areas with diverse land cover changes. Therefore, small subregions, which cover a range of land cover change intensities, are chosen to reflect local climate impacts due to different land cover changes.

Moreover, the FNFI data only covers the land surface in Finland without considering inland lakes. Therefore, the land sea mask in the model domain is adopted from CLC (2006). In addition, the land cover conditions of the area outside Finland in the model domain are the same as those, i.e., based on CLC (2006) and GLCCD, in Gao et al. (2014) and thus identical in both simulations.

2.3

In order to make the land surface parameters more suitable for this study, several modifications in REMO LSS

were done. Details of those modifications are documented in Appendix B.

3 Experiment design

Two simulations were conducted with the FNFI1 and FNFI10 land cover maps representing the land cover conditions before and after peatland forestation activities in Finland, respectively. The simulations were driven with 6 hourly lateral boundary conditions from ECWMF ERA-Interim reanalysis data (Simmons et al., 2007) from 1 January 1979 to 31 December 1996. The 18-year forward runs were preceded by 10-year (1 August 1979–1 January 1990) simulations in order to stabilise the deep soil temperatures and soil moistures. The last 15-year (1 December 1981–30 November 1996) out of the 18-year forward simulations were adopted for further analysis. The analysed period starts from 1 December in order to keep all the three winter months continuous. The simulated first one-and-a-half years were excluded in order to minimise the influences of the initial boundary conditions on simulated climate conditions, which have a much quicker adaptation speed than deep soil temperature. The model grid is in an 18 km resolution horizontally and extends over 27 vertical levels (up to 25 km). The model time step was set to 90 s and the time steps of output variables are 6 hourly for 3-D variables and hourly for 2-D variables. Daily data covering 24 h is processed from 18:00 UTC of previous day to 17:00 UTC of the current day. For 6 hourly data, 18:00 UTC of the previous day and 00:00 UTC, 06:00 UTC and 12:00 UTC of the current day were used for daily values. For this study domain, the growing season and the dormancy season cover the period from May to October and from November to April, respectively.

4 Results

The land cover change effects on regional climate conditions in Finland are analysed based on the differences in climate variables between the post-drainage and pre-drainage simulations (FNFI10 – FNFI1). This "delta change approach" is adopted to eliminate the uncertainties related to model bias (Gálos et al., 2011; Jacob et al., 2008).

4.1 Effects on climate over Finland

The differences in monthly averaged daily mean two-metre air temperature ($T_{2\,\mathrm{m}}$) are quite heterogeneous temporally and spatially. $T_{2\,\mathrm{m}}$ differences are most prominent in springtime and summertime (Fig. 3). The most noticeable difference in $T_{2\,\mathrm{m}}$, up to 0.43 K, takes place in the most intensive peatland forestation area in the middle west of Finland in April. The warming is also evident in February and March, with differences of 0.2 K in this area. However, $T_{2\,\mathrm{m}}$ turns to show a slight cooling, generally less than 0.1 K, in a few parts of this area from May to October. There are also two regions in northern Finland that show opposite changes compared to the peatland forestation area in the middle west of Finland with cooling in spring and warming in the growing season. This is because of decreased forest cover and increased fraction of Peat Bogs in those two areas from FNFI1 to FNFI10 based land cover maps. An increase of less than 0.2 K is seen in $T_{2\,\mathrm{m}}$ in the southeast of Finland in July and August, as well as in the very south of Finland throughout the growing season, which are mainly due to the change from Mixed Forest to Coniferous Forest and the increased Artificial Areas, respectively. The 15-year averaged monthly precipitation shows only small differences, less than 10 mm month^{-1}, in varied patterns in the model domain from April to August (not shown).

The snow clearance day is also an important indicator of springtime climate change in high-latitudes (Peng et al., 2013). Therefore, the snow clearance day for each gridbox in Finland is determined for the 15 years. The snow clearance day is defined here as the first day after which the total number of snow-covered days does not exceed the total number of snow-free days, and the selection of this day ends before midsummer in a year. The differences between the 15-year averaged snow clearance days of the two simulations (Fig. 4) show almost the same pattern as the differences in $T_{2\,\mathrm{m}}$ in April (Fig. 3). In the peatland forestation area in the middle west of Finland, the snow clearance days are mostly advanced from 0.5 to 3 days and in a few gridboxes advanced by up to 5 days in the 15-year mean. The two small areas in the north of Finland with reverse land cover changes in comparison to peatland forestation show up to two-day delays in general. In the very south of Finland, the snow clearance days are also generally advanced in accordance with the warming seen in $T_{2\,\mathrm{m}}$, but delayed in several scattered gridboxes, due to increased fraction of Artificial Areas at the expense of forests.

4.2 Effects on climate over five subregions

$T_{2\,\mathrm{m}}$ and precipitation, as well as several closely related climate variables (surface albedo, net surface solar radiation, snow depth, ET) for the five subregions were processed into 11 day running means to reduce the influence of day-to-day variations. The differences between the simulations in each of the regionally averaged climate variables were further averaged over the 15 years (Fig. 5). Herein, the date information (day of year, DOY) represents the middle contributing day of the 11 day averaging period.

$T_{2\,\mathrm{m}}$ of subregion1 shows a warming of 0.1 K to 0.2 K from February till the end of March, and an evident peak of increase from early April to early May (from DOY 95 to DOY 125), which reaches a maximum of 0.5 K in late April. $T_{2\,\mathrm{m}}$ of subregion2 has the same development as subregion1 throughout the whole year, but the warming is much smaller and the biggest difference occurs in the beginning of April being only 0.12 K. This is consistent with the differences in snow depth. The snow-cover period in subregion2 is shorter along with an earlier maximum difference in snow depth. Moreover, those characteristics of the differences in snow depths are in agreement with the differences in surface albedo qualitatively because snow is the key factor that controls the surface albedo in the snow-cover period. From the beginning of May to the beginning of October, $T_{2\,\mathrm{m}}$ turns to show a cooling of less than 0.1 K in subregion1 and subregion2, because the cooling caused by ET exceeds the warming caused by the slightly lower albedo. The variability of the differences in net surface solar radiation in the growing season is induced by the variability of cloud cover rather than surface albedo. In November, December and January, the differences in $T_{2\,\mathrm{m}}$ vary in both directions. In high-latitudes, incoming solar radiation is quite small and cloud cover fraction is high in late autumn and winter. Therefore, the differences in surface albedo are not able to induce differences in net surface solar radiation in this period. Instead, the surface air temperature is sensitive to changes in the long-wave radiation balance that may lead to atmospheric air temperature inversion under a clear sky, manifesting itself as extreme cold surface air temperature. Thus, the variability of the differences in cloud cover caused by short-term variations in the climate contributes to the varied differences in $T_{2\,\mathrm{m}}$ in this period.

The differences in $T_{2\,\mathrm{m}}$ for subregion3 show a warming of less than 0.1 K from DOY 91 to DOY 120, but also a warming in an even smaller magnitude throughout the growing season. The difference in surface albedo in subregion3 is close to 0, although the difference in snow depth is similar to that of subregion2 but with a time lag of around 15 days in the most intensive point. In subregion4, the snow depth shows a quite small increase from the beginning of January till the end of March, which is consistent with the increase in surface albedo and explains the slight decrease of up to 0.1 K in $T_{2\,\mathrm{m}}$, from the middle of February till the end of March. Subregion5 displays the opposite characteristics compared to subregion1 and subregion2 for all the investigated variables. The absolute differences in snow depth of subregion5 are smaller than those of subregion1, but larger than those of subregion2. Because subregion5 is located in the north of Finland, the biggest difference of snow depth occurs later than that of subregion1. The magnitude of the maximum differences in $T_{2\,\mathrm{m}}$ in snow-cover period of subregion5 also lies between that of subregion1 and subreigon2 and happens later than that of subregion1.

The differences of $T_{2\,\mathrm{m}}$ in the growing season depend on the surplus of energy balance terms, where ET manifests itself as latent heat flux. In general, the increase of ET amount in subregion2 is slightly higher than that in subregion1. As a consequence, the decrease of $T_{2\,\mathrm{m}}$ in subregion2 is slightly larger than that in subregion1 during the growing season when the albedo difference is quite small. The decreased ET and the slightly decreased surface albedo together result in a slight warming in the growing season in the other subregions. The extents of warming in the other subregions follow the magnitudes of the decreased ET because the differences in surface albedo are almost the same in the growing season.

Precipitation has higher variability than ET throughout the year in the five subregions. In general, the differences in precipitation are much larger in the growing season than in the dormancy season, when they are close to $0\,\mathrm{mm\,day^{-1}}$. In the growing season, the increase in precipitation of subregion1 occurs during a longer period and has a larger magnitude than that of subregion2. There are slight increases in the precipitation in subregion3 and also in subregion4, whereas the precipitation of subregion5 shows a decreasing tendency in the growing season, with the biggest differences less than 0.2 mm day^{-1}.

Furthermore, the maximum and minimum differences of gridpoint-wise and regionally averaged 11 day running mean of $T_{2\,\text{m}}$ over 15 years for subregion1 were investigated as complements for the regionally averaged 15-year mean differences (Fig. 6). $T_{2\,\text{m}}$ shows a maximum difference in gridpoint-wise of nearly 2 K in the snow-melting period over the 15 years, which is 1 K higher than the maximum difference in regionally averaged $T_{2\,\text{m}}$ over the 15 years and four times as much as that in the 15-year mean of regionally averaged $T_{2\,\text{m}}$. The timings of the three kinds of maximum differences in spring deviate from each other from 3 to 10 days. The minimum differences show only a small deviation between the gridpoint-wise and regional mean values over the 15 years. During the snow-melting period, the minimum differences of regionally averaged $T_{2\,\text{m}}$ is above 0, but not the gridpoint-wise $T_{2\,\text{m}}$. The springtime differences between regional mean and gridpoint-wise extremes elucidate that, even within one subregion with homogenous characteristics related to peatland forestation, the spring warming of $T_{2\,\text{m}}$ is temporally and spatially heterogeneous. This implies that local effects are more pronounced than the regional and temporal statistics can reveal. For the rest of the year, the differences between the maximum (minimum) of the gridpoint-wise and regionally averaged $T_{2\,\text{m}}$ are small and of more regional nature. In the period between November and January, the large variations of maximum (minimum) $T_{2\,\text{m}}$ are contributed by the inversion effects due to short-term variations in the climate.

Additionally, for a more thorough understanding of the relationships between spring warming and albedo changes in the snow-cover period due to peatland forestation, two correlation relationships were investigated over all the 15 years for subregion1 (Fig. 7). One is between the maximum temperature difference day (DOY) and the maximum surface albedo difference day (DOY). The other is between the inflection day of total albedo (the day when surface albedo just finishes a fast decrease from its wintertime level; DOY) and the snow clearance day (DOY). The maximum temperature difference days match with maximum albedo difference days in 6 years, and the rest of the years generally show a delayed maximum temperature difference day compared to the maximum albedo difference day, with a maximum deviation of 14 days. In general, the snow clearance day correlates well with the inflection point of surface albedo. For most years, the differences are less than 6 days, but three years show differences up to around 20 days. In those years, sporadic snowfall with a small accumulated snow depth cannot really introduce differences in total surface albedo over the subregion but influences the determination of the snow clearance day.

5

4.1 Relationships between the changes in biogeophysical aspects and the impacts on climate

To assess the generality of the causal relationships between land cover changes and climate variables, the spatial correlations between changes in the two surface energy balance relevant variables, surface albedo and ET, and $T_{2\mathrm{m}}$ are investigated. Consequently, the spatial correlations between changes in surface albedo and ET and changes in the surface parameter values are also explored. The correlations with fractional green vegetation cover is not shown in Fig. 8, because LAI and green vegetation ratio are both modulated with the monthly varying growth factor by the same scheme, and they are highly correlated (pearson correlation coefficient, r^2=0.984 for March, r^2=0.674 for June). Monthly means of 15- year averaged changes in March and June are selected to represent springtime and summertime, respectively. The changes in $T_{2\mathrm{m}}$ are in accordance with the changes in surface albedo in March (Fig. 8, **a**), which is almost linearly correlated with the changes in LAI (Fig. 8, **c**) and forest ratio (Fig. 8, **e**). The changes in $T_{2\mathrm{m}}$ are linearly correlated with the changes in ET over most of the area in June (Fig. 8, **b**). In general, the changes in ET are also correlated with the changes in LAI (Fig. 8, **d**), roughness length (Fig.8, **f**) and forest ratio (yearly-constant, not shown), despite the influences from drought that may happen in late summer. Overall, the changes in surface albedo and ET are closely dependent on the changes in land surface parameters, which are induced by the changes in fractional coverages of land cover types in the five subregions (Table 1). The changes in $T_{2\mathrm{m}}$ are mainly modulated by the changes in surface albedo and ET in spring and summer, respectively. Some gridboxes located in the southeast of Finland, where mixed forest was substituted by coniferous forest mainly, show deviations in the correlations with LAI (marked by yellow circles in Fig. 8, **b**, **c**, **d**). In this area, LAI increased with almost no change in forest ratio, which lead to relatively smaller decrease in surface albedo compared to other areas with the same magnitude of changes in LAI in March; the ET-induced cooling is outweighted by the albedo-induced warming, which causes a slight warming in June. In the following summer months, July and August, the ET-induced cooling typically gets smaller because of surface water limitation and consequent warming.

5 Discussion

5.1 Biogeophysical impacts of peatland forestation on regional climate

Surface albedo shows a notable decrease in peatland forestation areas during snow-cover period and a slight decrease in the growing season, whereas LAI, roughness length, fractional green vegetation cover and forest ratio increase throughout the year after peatland forestation. Those changes lead to an increase in springtime $T_{2\mathrm{m}}$, which occurs locally in accordance with the decrease in surface albedo. In the growing season, an increase in ET related to the increased LAI and fractional green vegetation cover leads to more energy consumed by latent heat flux than gained by slightly lower albedo. Additionally, higher roughness length can play a role by increasing turbulent mixing and consequently the magnitudes of turbulent fluxes. Thus, the scattered differences in precipitation in summer are contributed by more convective structures, while for the rest of the year the precipitation is basically controlled by large-scale meteorology. From the analysis of the results in the five subregions, the differences in the climate variables show that their magnitudes depend on the extent of land cover changes, while the timings of the extremes mostly depend on geographical locations (latitudes) that define the radiation balance through the seasonal cycle. Results also illustrate a positive feedback induced by peatland forestation between lower surface albedo and warmer $T_{2\,\mathrm{m}}$ in the snow-melting period. The warming caused by lower surface albedo in snow-cover period due to more forest leads to a quicker and earlier snow melting; meanwhile, the surface albedo is reduced and consequently the surface air temperature is increased. Additionally, the maximum difference in the gridpoint-wise 11 day running mean of $T_{2\,\mathrm{m}}$ in spring warming period over the 15 years reaches 2 K in subregion1, which is four times of the 15- year mean of the corresponding regionally averaged values. This illustrates that the spring warming effect from peatland forestation is highly heterogeneous spatially and temporally.

5.2 Comparison with observation based results

To examine the realism of the simulated effects on surface temperature in springtime from peatland forestation, linear temperature trends over 40 years (1959–1998) were calculated for March and April based on monthly mean daily maximum ($T_{2\mathrm{m},max}$) and monthly mean daily minimum ($T_{2\mathrm{m},min}$) surface temperatures over Finland from E-OBS gridded observational dataset in 0.25 degree resolution (Haylock et al., 2008) (Fig. 9). The significance of the trends was tested with the Student's t-test. Both $T_{2\mathrm{m},max}$ and $T_{2\mathrm{m},min}$ have increased in March and April during the 40 years, and the increases of temperatures in March are stronger than that in April. The major areas of peatland forestation, subregion1 and subregion2, are highlighted and statistically significant ($p<0.1$) in the trends of $T_{2\mathrm{m},max}$ in both March and April but not shown in the trends of $T_{2\mathrm{m},min}$. In springtime, the trend of $T_{2\mathrm{m},max}$ is influenced by the albedo-induced temperature changes locally, while the trend of $T_{2\mathrm{m},min}$ is more related to the general climate change caused by global GHGs increases. Thus, the local effects in the trends of $T_{2\mathrm{m},max}$ suggest that our modeled results show qualitatively a good correspondence to observational data. However, it is difficult to compare the exact magnitudes and patterns of temperature changes because observational data contains contributions from other factors, for instance, the effects of climatic teleconnections from land cover changes in surrounding areas of Finland and short lived climate forces, such as aerosols and reactive trace gases (Pitman et al., 2009).

Furthermore, regional averaged difference in the simulated 11 day running mean net surface solar radiation of subregion1 (Fig. 5, **d**) agrees well with the observed differences in daily mean (1971-2000) net surface solar radiation (Fig.4 in Lohila et al. (2010)) between open peatland and forest sites located in southern and northern Finland. The maximum differences in the observed net surface solar radiation at nutrient-rich sites are 40-45 $\mathrm{W\,m^{-2}}$ (on DOY 70) in the south, and 80-90 $\mathrm{W\,m^{-2}}$ (on DOY 110) in the north of Finland. At nutrient-poor sites, the maximum differences are 30-40 $\mathrm{W\,m^{-2}}$ (on DOY 80) in the south, and 60-70 $\mathrm{W\,m^{-2}}$ (on DOY 115-120) in the north of Finland. The maximum difference in the simulated 11 day running mean net surface solar radiation averaged over subregion1 is 6.5 $\mathrm{W\,m^{-2}}$ (on DOY 107). The timing of the maximum difference in our simulated results, for subregion1, falls within the range of that in the observed data. The much smaller magnitude of the maximum difference in the simulated results could be explained by the fact that only around 20 % of the land was transformed from peatland to forests in subregion1. The maximum difference in net surface solar radiation is caused by the advanced snow clearance day due to peatland forestation. The differences in surface albedo is biggest between snow covered peatland surface and non-snow covered forest surface, i.e. the maximum difference of surface albedo is mostly dependent on snow albedo. Snow albedo has a negative linear correlation with forest ratio (Fig. B1). Assuming that the entire land of subregion1 would have been changed from peatland to forests, the maximum difference in net surface solar radiation could be estimated to be five times larger, i.e. 32.5 $\mathrm{W\,m^{-2}}$ which is within the range of observations. Moreover, the evolution of the differences in both simulated and observed net surface solar radiation in spring can be divided into three phases: a slow increase, a quick increase and a quick drop. For the simulated net surface solar radiation, the slow increase occurs from the beginning of January until the end of March, and appears to be mostly induced by the differences in snow depth on land cover classes. The following quick increase occurs in a much shorter period in April, within 10 to 20 days. The quick drop of the differences in net surface solar radiation follows the strong decrease of snow cover. The quick increase and quick drop are mainly attributed to snow melting, which is very sensitive to warmed air temperature. After that, the difference of net surface solar radiation is much smaller in the growing season. Strong variability of the net surface solar radiation differences in summertime can be attributed to the relatively short averaging time (15 years) that does not even out the impact of periods of high and low cloudiness.

5.3 Perspectives to improve land-atmosphere interactions modelling

Our results show that local climate changes due to peatland forestation in Finland can be mainly attributed to the impacts of changed surface albedo and ET on surface temperature, whereas no strong influences on precipitation is found. Future studies for improving understanding about biogeophysical impacts on regional climate of peatland forestation and other land cover or land use intensity changes could focus on the following issues: the parameterization of albedo, the soil hydrology scheme, and the implementation and the accuracy of land cover maps.

Although the maximum background albedo values of FNFI land cover classes in this study are broadly consistent with the summertime albedo values derived especially for two observation stations in Finland in Kuusinen et al. (2013), the estimated albedo for land cover classes in high-latitude areas show variations in a range of studies. The mean summertime albedo for Coniferous Forest is only 0.079 in Hollinger et al. (2010), while it is 0.119 in our study. We used a summertime albedo for Broad-leaved Forest of 0.146, which is higher than the albedo values for Deciduous in Kuusinen et al. (2013), but it is still lower compared to 0.156 for aspen in Betts and Ball (1997) and 0.152 for deciduous in Hollinger et al. (2010). The cropland albedo is 0.189 in Hollinger et al. (2010), and it is much higher than the cropland albedo of 0.156 used in our study. In the middle boreal zone of Finland, the albedo of Peat Bogs and the albedo of forest are, on average, 0.145 and 0.115 in Solantie (1988), respectively. Thus, compared to those values, our lower albedo for Peat Bogs and higher albedo for forest (even only considering Coniferous Forest) may underestimate the warming effect contributed by more absorbed solar radiation in non-snow covered period. However, it is hard to estimate the overall influence on surface temperature because ET may be enhanced from increased net surface solar radiation. Furthermore, even albedo values of the same land cover class could be different in different parts of Finland. In Solantie (1988), the mean albedo of barren bogs in southern Finland and of the concentric raised bogs in the middle of Finland is only 0.128. Recent studies show that forest albedo is influenced by stand density and understory in different sites (Bernier et al., 2011).

In wintertime, the snow albedo scheme is much more important than the background albedo in determining the surface albedo for high-latitudes. The snow albedo scheme in REMO does not adequately represent the complex conditions over forests, with the linear dependence on snow surface temperature. Snow properties and canopy conditions, such as snow water content, grain size and snow pack thickness, as well as impurities on the snow surface, have a strong influence on snow albedo (Wiscombe and Warren, 1980). Moreover, there is no vertical structure of forests in REMO where the process of snow intercepted by canopy is crucial (Roesch et al., 2001). The canopy of forests is also important in causing a night-time warming by the shelter effect in areas with successful peatland forestation after about 15 years (Venäläinen et al., 1999).

Besides, soil moisture affects ET and precipitation, thus playing a vital role in energy partition and futhermore influences surface temperature (Hagemann et al., 2013). The simple bucket soil moisture scheme used in this study is insufficient to represent the complex soil hydrological processes (Hagemann et al., 2014). Also, the subgrid variability of soil saturation within a model gridbox is taken into account as one-third times the model resolution in the simple bucket hydrology scheme in REMO LSS for this study, which is restricted by the 3 km resolution of the FNFI land cover maps. This can lead to underestimation of the surface runoff because the differences between the two surface parameters, W_{max} and W_{min} are smaller over the model domain compared to those when using a 10 times finer resolution to represent the subgrid hydrologic heterogeneity with GLCCD or CLC (2006).

Furthermore, land surface parameters are allocated according to distributions of land cover types in land surface scheme. Spatially more explicit land cover maps with a parameter set tailored for the study area could reduce the uncertainties in simulation results of climate models from the source.

5.4 Biogeochemical aspects related to peatland forestation

Peatland is a significant source of CH_4, and the CH_4 emission rate is sensitive to temperature, water table level, plant root depth and soil nutriention level, etc. (Melton et al., 2013; Turetsky et al., 2014; Lohila et al., 2010). After peatland forestation, the soil water table level goes down leading to increased CO_2 release at the expense of CH_4 release (Minkkinen and Laine, 2006). As time goes by, carbon sequestration by the tree growth and the formation of a new litter layer could compensate the carbon loss from peatland. Lohila et al. (2010) combined the radiative forcing effects from the differences of albedo and GHG fluxes due to peatland forestation at site-level, and showed net cooling at two soil nutrient-rich sites in the south and north and one soil nutrient-poor site in the south of Finland. Accounting for such local impacts in a regional climate model requires very sophisticated process descriptions and detailed parameterisation of soil properties.

The biogeophysical impacts of vegetation-climate feedbacks on climate are modest in comparion to the effects of increased GHGs for Europe, but local, regional and seasonal effects can be significant (Wramneby et al., 2010). However, studies with dynamic vegetation models under climate projections with increased GHGs indicate that more carbon will be gained to terrestrial ecosystems in high-latitudes by the end of this century (Fallon et al., 2012; Zhang et al., 2014). This is due to increase in woody plants that induce biogeophysical feedbacks with an earlier onset of growing season.

6 Summary

To get a clear picture of the peatland forestation effects on the climate in Finland is important for future forest management to consider economic aspects and global warming mitigation. In this paper, we investigated the long-term biogeophysical effects of peatland forestation on near-surface climate conditions in Finland by using a historical (1920s) and a present-day

(2000s) land-use map based on Finnish National Forest Inventory data in a regional climate model REMO. The differences between the two simulations in surface air temperature and precipitation were examined. The results show that peatland forestation induces a spring warming effect and a slight cooling effect in the growing season, but a varied pattern with less than 10 mm month^{-1} differences in precipitation over Finland from April to September. The temperature response in spring in simulation results is well in line with that seen in observational maps. In the most intensive peatland forestation area in the middle west of Finland, the monthly averaged daily mean surface air temperature shows a warming effect of around 0.2 K in February and March and up to 0.43 K in April, whereas a cooling effect of, in general, less than 0.1 K is found from May till October. Consequently, the snow clearance days in model gridboxes over that area are advanced up to 5 days in the mean of 15 years. Furthermore, a more detailed analysis was conducted on five subregions with decreased fractions of transformation from peatland to other land cover classes. The 11 day running means of simulated temperature, surface albedo, net surface solar radiation and snow depth, as well as precipitation and ET, were averaged over 15 years. Results show a positive feedback induced by peatland forestation between decreased surface albedo and increased surface air temperature in the snow-melting period. Overall, decreased albedo in the snow-melting period and increased ET in the growing period as a result of peatland forestation are the most important biogeophysical aspects that cause changes in surface air temperature. The extent of these climate effects depends on the intensity and geological locations of peatland forestation.

In the future, for the aim of getting a more precise assessment of the biogeophysical impacts of peatland forestation on regional climate conditions, more accurate land cover maps and land surface parameters are essential. Also, a more robust land surface scheme could enhance the representation of interactions between land surface and climate.

Appendix A: Methods in deriving FNFI land cover maps

The sample of FNFI1 (1921–1924) consisted of inventory lines oriented from southwest to northeast at a distance of 26 km across most parts of the country. The total length of measured lines was 13 348 km, and the total number of assessed land figures was 93 922. In the CLC-classification method, mean tree height and crown cover are two important criteria for classifying land-use classes. However, because crown cover was not measured in FNFI1, the growing stock volume corresponding to crown cover thresholds were estimated using naturally regenerated forests and unditched pine mires in FNFI9 (1996–2003) and in FNFI10 (2004–2010), according to vegetation zone, site type, mean height and dominant tree species. Afterwards, fractions of the ten land cover classes that were used in this study were derived for the FNFI1 sample in FNFI1 by considering land-use class, estimated growing stock volume classes, mean height, vegetation zone, site type and tree species composition.

For the interpolation, the FNFI1 sample lines were split into slices with 1 km intervals in a S-N direction. The fractions of the ten land cover classes in each slice on inventory line (1380 m on average) were then used in calculating sample variograms. These sample variograms are fitted into a variogram model to derive kriging predictions using the R version 2.15.2 package gstat (Pebesma, 2004; R Core Team, 2012). The block kriging was carried out separately for the fraction of each of the ten land cover classes with isotropic exponential (or spherical) variogram model and a block size of $50\,\mathrm{km} \times 50\,\mathrm{km}$. A raster map in 3 km resolution was then produced for the coverage of the ten land cover classes.

In FNFI10, a systematic cluster sample (more details can be found at http://www.metla.fi/ohjelma/vmi/vmi10-otanta-en.htm) of 69 388 plots was measured (Korhonen et al., 2013). The distance between clusters of plots (10–14 plots/cluster) varied between 5 km (in southern Finland) and 11 km (in northern Finland). The classification of FNFI10 dataset was processed in a similar way to the FNFI1 data, with the exception that crown cover thresholds for classifying land-use classes can be used directly in FNFI10 because it is assessed. To derive the $3\,\mathrm{km} \times 3\,\mathrm{km}$ grid map, the cluster means of the proportions of the ten land cover classes were first calculated and then the same interpolation method was used as for FNFI1.

Appendix B: Modifications in REMO LSS in this study

In order to allocate the surface parameters to appropriate land cover classes, the standard GLCCD land cover classes are related to the ten land cover classes in the FNFI maps through comparing the definitions of land cover classes (Table B1).

Most of the surface parameters follow the built-in parameter values. However, large deviations were found when comparing the parameterised albedo with the observed albedo. Moreover, the method for background albedo parameterisation is not suitable for land-use change studies because the vegetation albedo and the soil albedo maps are both derived from satellite albedo data that were measured in 2001–2004 with respect to land cover over that period. A new method, Land Use Character Shifts (LUCHS), has been proposed for land cover change studies (Preuschmann, 2012). It derives the annual background albedo cycle for certain land-use types in one region from good quality remote sensing datasets – a surface albedo dataset and a land cover mask – that are produced in the same time period. Unfortunately, LUCHS is not feasible for high-latitude areas, where snow cover prevents the possibility of deriving background albedo values from satellite albedo data. Hence, a simplified method is developed in this study to derive the background albedo values of the ten land cover classes in FNFI land cover maps. It is based on the assumption that the vegetation albedo map and the soil albedo map in current REMO LSS are feasible to describe the albedo values of the land cover condition in FNFI10, because the two datasets are overlapping in time. Therefore, the soil albedo and the vegetation albedo values, in model gridboxes that satisfy a requirement of 80 % coverage of one land cover class in FNFI10, are averaged to represent the soil and vegetation albedo values of that land cover class. The 80 % threshold was decreased to 50 % for Natural Grasslands, Peat Bogs and Artificial Areas, as none of the model gridboxes have an 80 % coverage of those land cover classes in Finland. The derived albedo values and the standard deviations for each land cover class in FNFI maps are shown in Table B2. The maximum background albedos, calculated based on the derived soil and vegetation albedo for FNFI land cover classes, are then compared with the summertime albedo of similar land cover classes for a southern (Hyytiälä; 61°51′ N and 24°17′ E) and a northern (Värriö; 67°48′ N and 27°52′ E) Finnish observation stations. The station values are estimated by a linear unmixing approach with the land-use and forestry maps in combination with the MODIS BRDF/albedo product (Kuusinen et al., 2013). The derived and observed albedo values show good agreement for Peat Bogs, Mixed Forest, Transitional Woodland/Shrub and Agricultural Areas, as well as for Artificial Areas. Although the maximum albedo values of Coniferous Forest and Broad-leaved Forest in this study are roughly around 0.01 higher than those in Kuusinen et al. (2013), they are reasonable for considering albedo differences between land cover classes. The three land cover classes (Natural Grasslands, Moors and heathland, Open Spaces) are not found at the two stations; however, they take up only small proportions in the FNFI land cover maps.

The snow albedo scheme for calculating the surface albedo during snow-cover period was also found to require some improvements. When there is snow on the ground, the surface albedo in REMO LSS is a function of background albedo, snow albedo and snow depth. The snow albedo depends linearly on snow surface temperature and fr (Kotlarski, 2007). Based on previous studies (Køltzow, 2007; Räisänen et al., 2014; Roesch et al., 2001), the minimum snow albedo at snow surface temperature $T = 0\,°C$ (a_{min}) and the maximum snow albedo at snow surface temperature $T \leq -10\,°C$ (a_{max}) of non-forested area (fr = 0) in this study were increased from 0.4 to 0.56 and decreased from 0.8 to 0.68, respectively; in addition, the a_{min} and a_{max} of fully forested area (fr = 1) were both decreased to 0.25 (Fig. B1). For descriptions of the dynamics of snow cover, the interested reader is referred to (Kotlarski, 2007).

Moreover, the three parameters for describing the subgrid heterogeneity of soil hydrology (Hagemann and Gates, 2003), Beta, W_{min} and W_{max} were calculated in a subgrid scale of 6 km resolution. It is one-third of the 18 km REMO resolution. The reason for this is that the spatial resolution of the FNFI land cover maps is three times lower compared to that of the default GLCCD land cover map.

Corrections were also made to some of the surface parameters of Coniferous Forest and Mixed Forest, to obtain a better mutual consistency of the surface parameters for the three forest types. For Coniferous Forest, the fractional green vegetation cover in the dormancy season and in the growing seasons and the forest ratio were set to 0.91, 0.91, 0.8, respectively, as proposed for Fennoscandia by Claussen et al. (1994). For Mixed Forest, the fractional green vegetation cover and LAI in the dormancy season were revised to be half of those parameters in the growing season.

Table B1. Translations between the ten land cover classes in FNFI maps and GLCCD land cover classes.

FNFI Class	Legend	GLCCD Class	Legend
1	Coniferous Forest	21	Conifer Boreal Forest
2	Mixed Forest	23	Cool Mixed Forest
3	Broad-leaved Forest	25	Cool Broadleaf Forest
4	Artificial Areas	30	Cool Crops and Towns
5	Natural Grasslands	40	Cool Grasses and Shrubs
6	Peat Bogs	44	Mire, Bog, Fen
7	Open Spaces	53	Barren Tundra
8	Transitional Woodland/Shrub	62	Narrow Conifers
9	Moors and heathland	64	Heath Scrub
10	Agricultural Areas	93	Grass Crops

Table B2. Derived soil albedo and vegetation albedo values with standard deviations for the land cover classes in the FNFI maps, and the threshold used for each land cover class; the minimum and maximum background albedo values (with standard deviations) in the yearly cycle calculated based on the derived soil and vegetable albedo values are also shown, as well as the summertime albedo values (i.e. maximum background albedo values) of the corresponding land cover classes observed at two Finnish stations (Hyytiälä, Värriö) in Kuusinen et al. (2013).

Class	Legend	Threshold (%)	Mean soil albedo ± SD	Mean vegetation albedo ± SD	Maximum albedo ± SD	Minimum albedo ± SD	Maximum(Hyytiälä) albedo ± SD	Maximum(Värriö) albedo ± SD
1	Coniferous Forest	80	0.091 ± 0.017	0.121 ± 0.011	0.119 ± 0.012	0.119 ± 0.012	0.102 ± 0.004	0.108 ± 0.004
2	Mixed Forest	80	0.077 ± 0.003	0.134 ± 0.022	0.128 ± 0.020	0.119 ± 0.017	–	0.116 ± 0.005
3	Broad-leaved Forest	80	0.091 ± 0.007	0.151 ± 0.001	0.146 ± 0.001	0.112 ± 0.005	0.143 ± 0.005	0.137 ± 0.005
4	Artificial Areas	50	0.090 ± 0.000	0.167 ± 0.000	0.145 ± 0.000	0.114 ± 0.000	0.147 ± 0.007	0.120 ± 0.008
5	Natural Grasslands	50	0.074 ± 0.000	0.211 ± 0.004	0.155 ± 0.002	0.077 ± 0.000	–	–
6	Peat Bogs	50	0.129 ± 0.054	0.133 ± 0.011	0.132 ± 0.023	0.129 ± 0.052	0.140 ± 0.011	0.134 ± 0.006
7	Open Spaces	80	0.147 ± 0.013	0.128 ± 0.001	0.136 ± 0.007	0.147 ± 0.013	–	–
8	Transitional Woodland/Shrub	80	0.074 ± 0.003	0.131 ± 0.008	0.120 ± 0.007	0.076 ± 0.004	0.126 ± 0.004	0.128 ± 0.006
9	Moors and heathland	80	0.124 ± 0.001	0.144 ± 0.001	0.142 ± 0.001	0.125 ± 0.001	–	–
10	Agricultural Areas	80	0.087 ± 0.011	0.184 ± 0.011	0.156 ± 0.011	0.128 ± 0.011	0.150 ± 0.006	–

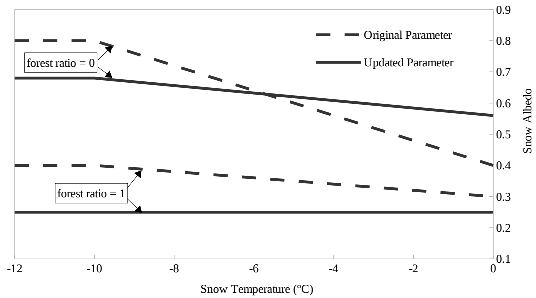
Original Parameter
Updated Parameter
forest ratio = 0
forest ratio = 1
0.9
0.8
0.7
0.6
0.5
0.4
0.3
0.2
0.1
Snow Albedo
-12
-10
-8
-6
-4
-2
0
Snow Temperature (°C)

Figure B1. Modified snow albedo values in the snow albedo scheme (modified based on Fig. 3.6 in Kotlarski (2007)).

Acknowledgement. The study was funded by Helsinki University Centre for Environment (HENVI), and supported by the Academy of Finland's Centers of Excellence (project no 272041). We are also grateful to Stefan Weiher from Brandenburg Technical University, Germany, and Stefan Hagemann from Max Planck Institute for Meteorology, Germany, for their valuable comments on this work. We acknowledge the E-OBS dataset from the EU-FP6 project ENSEMBLES (http://ensembles-eu.metoffice.com) and the data providers in the ECAD project (http://www.ecad.eu).

References

Bala, G., Caldeira, K., Wickett, M., Phillips, T. J., Lobell, D. B., Delire, C., and Mirin, A.: Combined climate and carbon-cycle effects of large-scale deforestation, P. Natl. Acad. Sci. USA, 104, 6550–6555, 2007.

Bathiany, S., Claussen, M., Brovkin, V., Raddatz, T., and Gayler, V.: Combined biogeophysical and biogeochemical effects of large-scale forest cover changes in the MPI earth system model, Biogeosciences, 7, 1383–1399, doi:10.5194/bg-7-1383-2010, 2010.

Bernier, P. Y., Desjardins, R. L., Karimi-Zindashty, Y., Worth, D., Beaudoin, A., Luo, Y., and Wang, S.: Boreal lichen woodlands: a possible negative feedback to climate change in eastern North America, Agr. Forest Meteorol., 151, 521–528, 2011.

Betts, A. K. and Ball, J. H.: Albedo over the boreal forest, J. Geophys. Res.-Atmos., 102, 28901–28909, 1997.

Betts, R. A.: Offset of the potential carbon sink from boreal forestation by decreases in surface albedo, Nature, 408, 187–190, 2000.

Betts, R. A., Falloon, P. D., Goldewijk, K. K., and Ramankutty, N.: Biogeophysical effects of land use on climate: model simulations of radiative forcing and large-scale temperature change, Agr. Forest Meteorol., 142, 216–233, 2007.

Bonan, G. B.: Forests and climate change: forcings, feedbacks, and the climate benefits of forests, Science, 320, 1444–1449, 2008.

Claussen, M., Lohmann, U., Roeckner, E., and Schulzweida, U.: A global data set of land-surface parameters, MPI Report No. 135, Max Planck Institute for Meteorology, Hamburg, Germany, 33 pp., 1994.

Déqué, M., Jones, R. G., Wild, M., Giorgi, F., Christensen, J. H., Hassell, D. C., Vidale, P. L., Rockel, B., Jacob, D., Kjellström, E., De Castro, M., Kucharski, F., and Van den Hurk, B.: Global high resolution versus Limited Area Model climate change projections over Europe: quantifying confidence level from PRUDENCE results, Clim. Dynam., 25, 653–670, doi:10.1007/s00382-005-0052-1, 2005.

Davies, H. C.: A laterul boundary formulation for multi-level prediction models, Q. J. Roy. Meteor. Soc., 102, 405–418, 1976.

Dümenil, L. and Todini, E.: A rainfall-runoff scheme for use in the Hamburg climate model, in: Advances in Theoretical Hydrology-a Tribute to James Dooge, European Geophysical Society Series on Hydrological Sciences, 1, edited by: O'Kane, J. P., Elsevier Science, Amsterdam, The Netherlands, 9, 129–157, 1992.

Falloon, P. D., Dankers, R., Betts, R. A., Jones, C. D., Booth, B. B. B., and Lambert, F. H.: Role of vegetation change in future climate under the A1B scenario and a climate stabilisation scenario, using the HadCM3C Earth system model, Biogeosciences, 9, 4739-4756, 2012.

FAO/UNESCO: Soil Map of the World, UNESCO, Paris, 1971–1981.

Feddema, J. J., Oleson, K. W., Bonan, G. B., Mearns, L. O., Buja, L. E., Meehl, G. A., and Washington, W. M.: The importance of land-cover change in simulating future climates, Science, 310, 1674–1678, 2005.

Gálos, B., Mátyás, C., and Jacob, D.: Regional characteristics of climate change altering effects of afforestation, Environ. Res. Lett., 6, 044010, doi:10.1088/1748-9326/6/4/044010, 2011.

Göttel, H., Alexander, J., Keup-Thiel, E., Rechid, D., Hagemann, S., Blome, T., Wolf, A., and Jacob, D.: Influence of changed vegetations fields on regional climate simulations in the Barents Sea Region, Climatic Change, 87, 35–50, 2008.

Gao, Y., Weiher, S., Markkanen, T., Pietikäinen, J.-P., Gregow, H., Henttonen, H. M., Jacob, D., and Laaksonen, A.: Implementation of the CORINE land use classification in the regional climate model REMO, Boreal Environ. Res., accepted, 2014.

Ge, J. and Zou, C.: Impacts of woody plant encroachment on regional climate in the southern Great Plains of the United States, J. Geophys. Res.-Atmos., 118, 9093–9104, 2013.

Hökkä, H., Kaunisto, S., Korhonen, K. T., Päivänen, J., Reinikainen, A., and Tomppo, E.: Suomen suometsät 1951–1994, Metsätieteen aikakauskirja, 2B, Finnish Forest Research Institute, Helsinki, Finland, 201–357, 2002.

Hagemann, S.: An improved land surface parameter dataset for global and regional climate models, MPI Report No. 336, Max Planck Institute for Meteorology, Hamburg, Germany, 17 pp., 2002.

Hagemann, S. and Gates, L. D.: Improving a subgrid runoff parameterization scheme for climate models by the use of high resolution data derived from satellite observations, Clim. Dynam., 21, 349–359, 2003.

Hagemann, S., Botzet, M., Dümenil, L., and Machenhauer, B.: Derivation of global GCM boundary conditions from 1 KM land use satellite data, MPI Report No. 289, Max Planck Institute for Meteorology, Hamburg, Germany, 34 pp., 1999.

Hagemann, S., Loew, A., and Andersson, A.: Combined evaluation of MPI-ESM land surface water and energy fluxes, J. Adv. Model. Earth Syst., 5, 259–286, 2013.

Hagemann, S., Stacke, T.: Impact of the soil hydrology scheme on simulated soil moisture memory, Clim. Dynam., 1-20, doi:10.1007/s00382-014-2221-6, 2014.

Haylock, M. R., Hofstra, N., Klein Tank, A. M. G., Klok, E. J., Jones, P. D., and New., M.: A European daily high-resolution gridded dataset of surface temperature and precipitation, J. Geophys. Res-Atmos., 113, D20119, doi:10.1029/2008JD10201, 2008.

Hollinger, D. Y., Ollinger, S. V., Richardson, A. D., Meyers, T. P., Dail, D. B., Martin, M. E., Scott, N. A., Arkebauer, T. J., Baldocchi, D. D., Clark, K. L., Curtis, P. S., Davis, K. J., Desai, A. R., Dragoni, D., Goulden, M. L., Gu, L., Katul, G. G., Pallardy, S. G., Paw U, K. T., Schmid, H. P., Stoy, P. C., Suyker, A. E., and Verma, S. B.: Albedo estimates for land surface models and support for a new paradigm based on foliage nitrogen concentration, Glob. Change Biol., 16, 696–710, 2010.

Ilvessalo, Y.: Suomen metsät. Tulokset vuosina 1921–1924 suoritetusta valtakunnan metsien arviomisesta (summary in english: the forests of Finland. Results of the general survey of the forests of the country carried out during the years 1921–1924), Communicationes ex Instituto Quaestionum Forestalium Finlandiae 11, Valtioneuvoston kirjapaino, 1927.

Ilvessalo, Y.: Suomen metsät vuosina 1921–24 vuosiin 1951–53: kolmeen valtakunnan metsien inventointiin perustuva tutkimus (the forests of Finland from 1921–24 to 1951–53. A survey based on three national forest inventories), Communicationes Instituti Forestalis Fenniae, Finnish Forest Research Institute, Helsinki, Finland, 47, 277 pp., 1956.

IPCC: Climate Change 2013: The Physical Science Basis. Working Group 1 Contribution to the Fifth Assessment Report of the Intergovernmental Panel on Climate Change, Cambridge, UK and New York, NY, USA, 1535 pp., 2013.

Jacob, D. and Podzun, R.: Sensitivity studies with the regional climate model REMO, Meteorol. Atmos. Phys., 63, 119–129, 1997.

Jacob, D., Van den Hurk, B. J. J. M., Andrae, U., Elgered, G., Fortelius, C., Graham, L. P., Jackson, S. D., Karstens, U., Köpken, Chr., Lindau, R., Podzun, R., Rockel, B., Rubel, F., Sass, B. H., Smith, R. N. B., and Yang, X.: A comprehensive model inter-comparison study investigating the water budget during the BALTEX-PIDCAP period, Meteorol. Atmos. Phys., 77, 19–43, 2001.

Jacob, D., Bärring, L., Christensen, O. B., Christensen, J. H., De Castro, M., Déqué, M., Giorgi, F., Hagemann, S., Hirschi, M., Jones, R., Kjellström, E., Lenderink, G., Rockel, B., Sánchez, E., Schär, C., Seneviratne, S. I., Somot, S., Van Ulden, A., and Van den Hurk, B.: An intercomparison of regional climate models for Europe: model performance in present-day climate, Climatic Change, 81, 31–52, doi:10.1007/s10584-006-9213-4, 2007.

Jacob, D., Kotova, L., Lorenz, P., Moseley, C., and Pfeifer, S.: Regional climate modeling activities in relation to the CLAVIER project, Idöjárás, 112, 141–153, 2008.
Køltzow, M.: The effect of a new snow and sea ice albedo scheme on regional climate model simulations, J. Geophys. Res.-Atmos., 112, D07110, doi:10.1029/2006JD007693, 2007.
Kaakinen E. and Salminen, P.: Mire conservation and its short history in Finland, in: Finland – land of mires, The Finnish Environment, 23, edited by: Lindholm, T. and Heikkilä, R., Finnish Environment Institute, Helsinki, Finland, 229–238, 2006.
Korhonen, K. T., Ihalainen, A., Viiri, H., Heikkinen, J., Henttonen, H. M., Hotanen, J. P., Mäkelä, H., Nevalainen, S., and Pitkänen, J.: Suomen metsät 2004–2008 ja niiden kehitys 1921–2008 (the forests of Finland in 2004–2008 and their development from 1921 to 2008), Metsätieteen aikakauskirja, 3, Finnish Forest Research Institute, Helsinki, Finland, 269–608, 2013.
Kotlarski, S.: A subgrid glacier parameterisation for use in regional climate modelling, Ph. D. thesis, University of Hamburg, Max Planck Institute for Meterology, Hamburg, Germany, 2007.
Kuusinen, N., Tomppo, E., and Berninger, F.: Linear unmixing of MODIS albedo composites to infer subpixel land cover type albedos, Int. J. Appl. Earth Obs., 23, 324–333, 2013.
Laiho, R., Vasander, H., Penttilä, T., and Laine, J.: Dynamics of plant-mediated organic matter and nutrient cycling following water-level drawdown in boreal peatlands, Global Biogeochem. Cy., 17, 1053, 2003.
Laine, J., Vasander, H., and Laiho, R.: Long-term effects of water level drawdown on the vegetation of drained pine mires in southern Finland, J. Appl. Ecol., 32, 785–802, 1995.
Legates, D. R. and Willmott, C. J.: Mean seasonal and spatial variability in global surface air temperature, Theor. Appl. Climatol., 41, 11–21, 1990.
Lohila, A., Minkkinen, K., Laine, J., Savolainen, I., Tuovinen, J.-P., Korhonen, L., Laurila, T., Tietäväinen, H., and Laaksonen, A.: Forestation of boreal peatlands: impacts of changing albedo and greenhouse gas fluxes on radiative forcing, J. Geophys. Res.-Biogeo., 115, G04011, doi:10.1029/2010JG001327, 2010.
Loveland, T. R., Reed, B. C., Brown, J. F., Ohlen, D. O., Zhu, Z., Yang, L., and Merchant, J. W.: Development of a global land cover characteristics database and IGBP DISCover from 1 km AVHRR data, Int. J. Remote Sens., 21, 1303–1330, 2000.
Majewski, D.: The Europa-Modell of the Deutscher Wetterdienst, in: ECMWF Seminar on numerical methods in atmospheric models, 2 (Vol.), Reading, UK, 147–191, 1991.
Manabe, S.: Climate and the ocean circulation 1: I. The atmospheric circulation and the hydrology of earth's surface, Mon. Weather Rev., 97, 739–774, 1969.

McGregor, J.: Regional climate modelling, Meteorol. Atmos. Phys., 63, 105–117, 1997.
Metsätalouden kehittämiskeskus Tapio: Metsätalouden säädökset (Forestry regulations), Tapio, Finland, 111 pp., 1997.
Melton, J. R., Wania, R., Hodson, E. L., Poulter, B., Ringeval, B., Spahni, R., Bohn, T., Avis, C. A., Beerling, D. J., Chen, G., Eliseev, A. V., Denisov, S. N., Hopcroft, P. O., Lettenmaier, D. P., Riley, W. J., Singarayer, J. S., Subin, Z. M., Tian, H., Zürcher, S., Brovkin, V., van Bodegom, P. M., Kleinen, T., Yu, Z. C., and Kaplan, J. O.: Present state of global wetland extent and wetland methane modelling: conclusions from a model inter-comparison project (WETCHIMP), Biogeosciences, 10, 753-788, doi:10.5194/bg-10-753-2013, 2013.
Minkkinen, K. and Laine, J.: Vegetation heterogeneity and ditches create spatial variability in methane fluxes from peatlands drained for forestry, Plant and Soil, 285, 289-304, doi:10.1007/s11104-006-9016-4, 2006.
Minkkinen, K., Korhonen, R., Savolainen, I., and Laine, J.: Carbon balance and radiative forcing of Finnish peatlands 1900–2100 – the impact of forestry drainage, Glob. Change Biol., 8, 785–799, 2002.
Olson, J. S.: Global ecosystem framework-definitions, USGS EROS Data Center Internal Report, Sioux Falls, SD, 37 pp., 1994a.
Olson, J. S.: Global ecosystem framework-translation strategy, USGS EROS Data Center Internal Report, Sioux Falls, SD, 39 pp., 1994b.
Päivänen, J. and Hånell, B.: Peatland Ecology and Forestry: A Sound Approach, University of Helsinki Department of Forest Sciences Publication 3, Department of Forest Ecology, University of Helsinki, Helsinki, Finland, 2012.
Pebesma, E. J.: Multivariable geostatistics in S: the gstat package, Comput. Geosci., 30, 683–691, 2004.
Peng, S., Piao, S., Ciais, P., Friedlingstein, P., Zhou, L., and Wang, T.: Change in snow phenology and its potential feedback to temperature in the Northern Hemisphere over the last three decades, Environ. Res. Lett., 8, 014008, doi:10.1088/1748-9326/8/1/014008, 2013.
Pielke, R. A., Avissar, R., Raupach, M., Dolman, A. J., Zeng, X., and Denning, A. S.: Interactions between the atmosphere and terrestrial ecosystems: influence on weather and climate, Glob. Change Biol., 4, 461–475, 1998.
Pielke, R. A., Pitman, A., Niyogi, D., Mahmood, R., McAlpine, C., Hossain, F., Goldewijk, K. K., Nair, U., Betts, R., Fall, S., Reichstein, M., Kabat, P., and de Noblet, N.: Land use/land cover

changes and climate: modeling analysis and observational evidence, Wiley Interdisciplinary Reviews: Climate Change, 2, 828–850, 2011.
Pitman, A. J.: The evolution of, and revolution in, land surface schemes designed for climate models, Int. J. Climatol., 23, 479–510, 2003.
Pitman, A. J., de NobletDucoudré, N., Cruz, F. T., Davin, E. L., Bonan, G. B., Brovkin, V., Claussen, M., Delire, C., Ganzeveld, L., Gayler, V., van den Hurk, B. J. J. M., Lawrence, P. J., van der Molen, M. K., Müller, C., Reick, C. H., Seneviratne, S. I., Strengers, B. J., and Voldoire, A.: Uncertainties in climate responses to past land cover change: First results from the LUCID intercomparison study, Geophysical Research Letters, 36, L14814, doi:10.1029/2009GL039076, 2009.
Preuschmann, S.: Regional surface albedo characteristics – analysis of albedo data and application to land-cover changes for a regional climate model, Ph. D. thesis, University of Hamburg, Max Planck Institute for Meterology, Hamburg, 2012.
R Development Core Team, R: A Language and Environment for Statistical Computing, The R Foundation for Statistical Computing, Vienna, Austria, 2011.
Räisänen, P., Luomaranta, A., Järvinen, H., Takala, M., Jylhä, K., Bulygina, O. N., Riihelä, A., Laaksonen, A., Koskinen, J., and Pulliainen, J.: Evaluation of North Eurasian snow-off dates in the ECHAM5.4 atmospheric GCM, Geosci. Model Dev. Discuss., 7, 3671–3715, doi:10.5194/gmdd-7-3671-2014, 2014.
Rechid, D.: On biogeophysical interactions between vegetation phenology and climate simulated over Europe, Ph. D. thesis, University of Hamburg, Max Planck Institute for Meterology, Hamburg, 2008.
Rechid, D. and Jacob, D.: Influence of monthly varying vegetation on the simulated climate in Europe, Meteorol. Z., 15, 99–116, 2006.
Rechid, D., Raddatz, T. J., and Jacob, D.: Parameterization of snow-free land surface albedo as a function of vegetation phenology based on MODIS data and applied in climate modelling, Theor. Appl. Climatol., 95, 245–255, 2009.
Roeckner, E., Arpe, K., Bengtsson, L., Christoph, M., Claussen, M., Dümenil, L., Esch, M., Giogetta, M., Schlese, U., and Schultz-Weida, U.: The Atmospheric General Circulation Model ECHAM4: Model Description and Simulation of the Present-Day Climate, MPI Report No. 218, Max Planck Institute for Meterology, Hamburg, Germany, 90 pp., 1996.
Roesch, A., Wild, M., Gilgen, H., and Ohmura, A.: A new snow cover fraction parametrization for the ECHAM4 GCM, Clim. Dynam., 17, 933–946, 2001.

Semmler, T., Jacob, D., Schlünzen, K. H., and Podzun, R.: Influence of sea ice treatment in a regional climate model on boundary layer values in the Fram Strait Region, Mon. Weather Rev., 132, 985–999, 2004.

Simmons, A., Uppala, S., Dee, D., and Kobayashi, S.: ERA-Interim: new ECMWF reanalysis products from 1989 onwards, ECMWF newsletter, 110, 25–35, 2007.

Solantie, R.: Albedo in Finland on the Basis of Observations on Aircraft, Meteorological publications, 12, Finnish Meterological Institute, Helsinki, Finland, 106 pp., 1988.

Solantie, R.: Suurten suo-ojitusten vaikutus ilman lämpötilaan erityisesti Alajärven Möksyn havaintojen perusteella (the impact of large scale wetland drainage on air temperature based on observations in Möksy in Alajärvi), Meteorological publications, 29, Finnish Meterological Institute, Helsinki, 40 pp., 1994.

Tomppo, E., Gschwantner, M., Lawrence, M., and McRoberts, R. E.: National Forest Inventories, Pathways for Common Reporting, Springer, The Netherlands, 2010.

Tomppo, E., Heikkinen, J., Henttonen, H. M., Ihalainen, A., Katila, M., Mäkelä, H., Tuomainen, H., and Vainikainen, N.: Designing and Conducting a Forest Inventory-case: 9th National Forest Inventory of Finland, Springer, The Netherlands, 2011.

Turetsky, M. R., Kotowska, A., Bubier, J., Dise, N. B., Crill, P., Hornibrook, E. R. C., Minkkinen, K., Moore, T. R., Myers-Smith, I. H., Nykänen, H., Olefeldt, D., Rinne, J., Saarnio, S., Shurpali, N., Tuittila, E.-S., Waddington, J. M., White, J. R., Wickland, K. P. and Wilmking, M.: A synthesis of methane emissions from 71 northern, temperate, and subtropical wetlands, Global change biology, 20, 2183-2197, doi:10.1111/gcb.12580, 2014.

US Geological Survey: Global land cover characteristics data base version 2.0, available at: http://edc2.usgs.gov/glcc/globdoc2_0.php, 2001.

Venäläinen, A., Rontu, L., and Solantie, R.: On the influence of peatland draining on local climate, Boreal Environ. Res., 4, 89–100, 1999.

Wiscombe, W. J. and Warren, S. G.: A model for the spectral albedo of snow. I: Pure snow, J. Atmos. Sci., 37, 2712–2733, 1980.

Wramneby, A., Smith, B., and Samuelsson, P.: Hot spots of vegetationclimate feedbacks under future greenhouse forcing in Europe, J. Geophys. Res.-Atmos., 115, D21119, doi:10.1029/2010JD014307, 2010.

Zhang, W., Jansson, C., Miller, P. A., Smith, B., and Samuelsson, P.: Biogeophysical feedbacks enhance Arctic terrestrial carbon sink in regional Earth system dynamics, Biogeosciences, 11, 5503-5519, doi:10.5149/bg-11-5503-2014, 2014.

Table 1. Changes of fractional coverage (%) of the ten land cover classes from the 1920s to the 2000s (FNFI10 – FNFI1) in the five subregions.

Class	Legend	Subregion1	Subregion2	Subregion3	Subregion4	Subregion5
1	Coniferous Forest	13.40	18.03	−2.24	−11.74	−10.13
2	Mixed Forest	1.23	−3.46	−2.30	−1.86	−2.10
3	Broad-leaved Forest	1.24	0.98	1.68	−0.52	−4.11
4	Artificial Areas	4.44	4.95	2.44	5.69	2.52
5	Natural Grasslands	−4.41	−2.10	−1.71	−2.82	−1.60
6	Peat Bogs	−22.92	−20.82	−12.60	−3.80	8.64
7	Open Spaces	0.06	−0.12	−0.11	−0.31	−1.14
8	Transitional Woodland/Shrub	3.64	−0.72	14.26	4.84	9.12
9	Moors and heathland	0.00	0.00	0.00	0.00	−1.37
10	Agricultural Areas	3.31	3.26	0.57	10.52	0.17

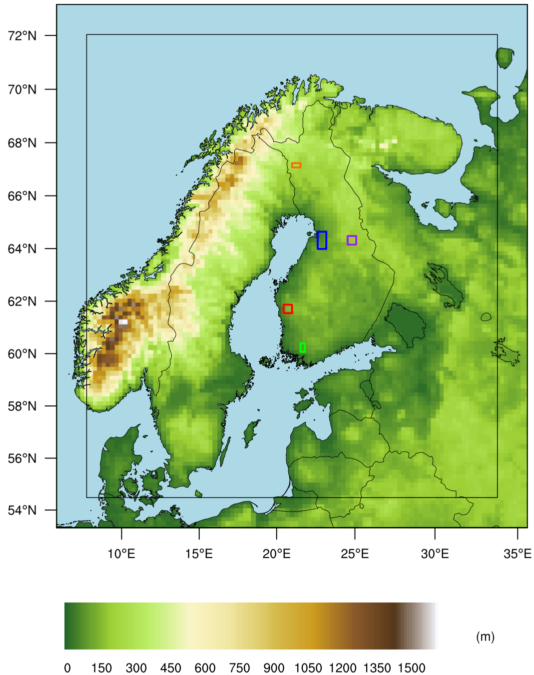

Figure 1. Orography of the model domain, and the five selected subregions (subregion1–blue; subregion2–red; subregion3–purple; subregion4–green; subregion5–orange). The inner black frame shows the extent of the relaxation zone from outer boundary, i.e. the eight outer most gridboxes in each direction of the model domain.

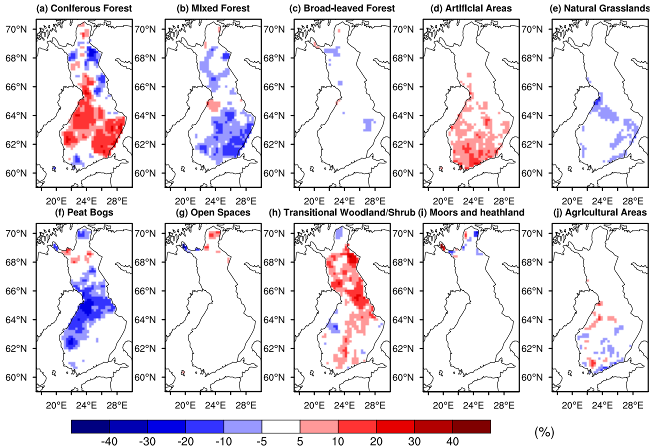

Figure 2. Changes of fractional coverage of the ten land cover classes in Finland from the 1920s to the 2000s (FNFI10 – FNFI1).

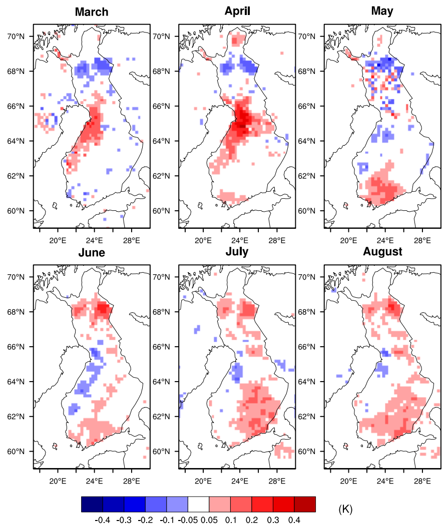

in spring and summer months.

0 The 15- year averaged differences (FNFI10 – FNFI1) in monthly averaged daily mean two-metre air temperature
in spring and summer months.

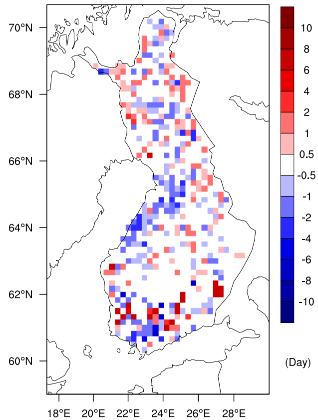

Figure 4. The 15-year averaged differences (FNFI10 – FNFI1) in the snow clearance days over model gridboxes in Finland.

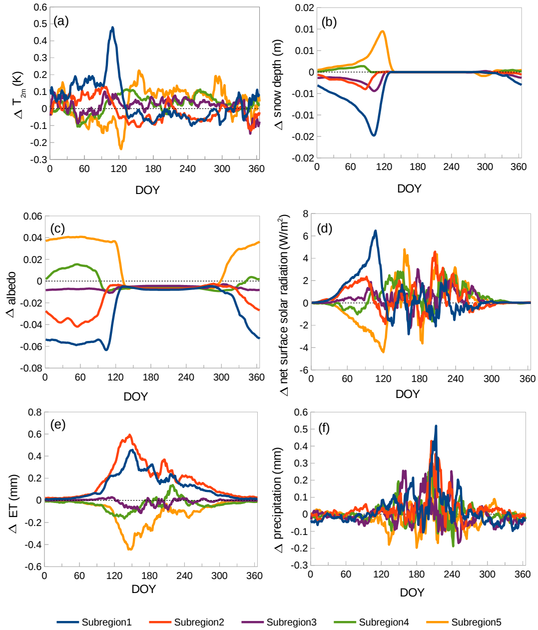

Figure 5. The 15-year averaged regional mean differences (FNFI10 – FNFI1) in 11 day running mean of daily mean (**a**) two-metre air temperature, (**b**) snow depth (presented as equivalent water), (**c**) surface albedo, (**d**) net surface solar radiation, (**e**) ET and (**f**) precipitation of the five subregions.

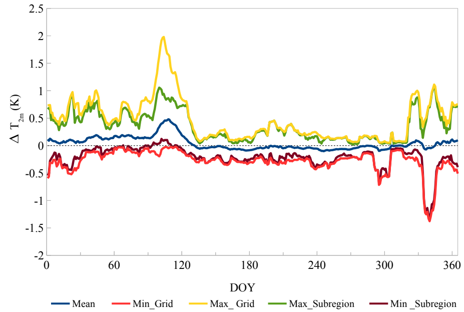

Figure 6. Maximum, minimum and mean differences of gridpoint-wise and regionally averaged 11 day running mean of daily mean two-metre air temperature over 15 years in subregion1.

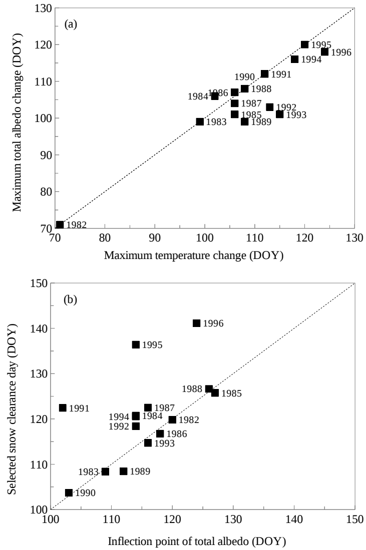

Figure 7. (a) Correlation between maximum temperature change day (DOY) and maximum total albedo change day (DOY); **(b)** correlation between inflection day of total albedo (the day when surface albedo just finishes a fast decrease from its wintertime level; DOY) and the snow clearance day (DOY). The plots show regional means over subregion1 for all 15 years.

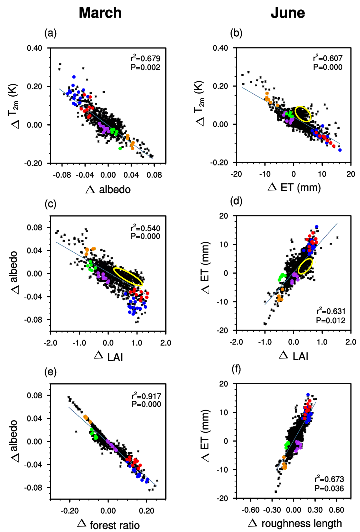

Figure 8. Spatial correlations between (**a**) changes in monthly averaged daily mean two-metre air temperature (T_{2m}) and changes in albedo for March, (**b**) changes in T_{2m} and changes in ET for June, and also relationships between changes in land surface parameters in REMO LSS following land cover changes and changes in albedo (**c**,**e**) (changes in ET (**d**,**f**)) in the corresponding month. The changes in the gridboxes in selected subregions are shown with coloured dots (subregion1–blue; subregion2–red; subregion3–purple; subregion4–green; subregion5–orange). The gridboxes in yellow circles show the changes in the southeast area of Finland.

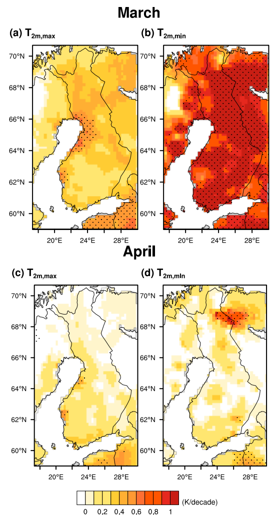

Figure 9. Temperature trends over 40 years (1959-1998) for (**a**,**c**) monthly mean daily maximum and (**b**,**d**) monthly mean daily minimum surface temperatures of March and April. The areas covered with black dots are statistical significant ($p<0.1$).